Stiff

NASA TECHNICAL MEMORANDUM

NASA TM X-62,433

LOW SPEED WIND TUNNEL TESTS ON A ONE-SEVENTH SCALE MODEL OF THE H.126 JET FLAP AIRCRAFT

Georgene H. Laub

Ames Directorate
U. S. Army Air Mobility R&D Laboratory
Moffett Field, Calif. 94035

April 1975

1. Report No.	2. Government Accession No.	3. Recipient's Catalog No.
TM X-62,433		

4. Title and Subtitle	5. Report Date
LOW SPEED WIND TUNNEL TESTS ON A ONE-SEVENTH SCALE MODEL OF THE H.126 JET FLAP AIRCRAFT	6. Performing Organization Code

7. Author(s)	8. Performing Organization Report No.
Georgene H. Laub	A-6074

9. Performing Organization Name and Address	10. Work Unit No.
Ames Directorate U. S. Army Air Mobility R&D Laboratory Moffett Field, Calif. 94035	505-10-21
	11. Contract or Grant No.
	13. Type of Report and Period Covered
12. Sponsoring Agency Name and Address	Technical Memorandum
National Aeronautics and Space Administration Washington, D. C. 20546	14. Sponsoring Agency Code

15. Supplementary Notes

16. Abstract

Low speed wind tunnel tests were performed on a one-seventh scale model of the British H.126 jet flap research aircraft over a range of jet momentum coefficients.

The primary objective was to compare model aerodynamic characteristics with those of the aircraft, with the intent to provide preliminary data needed towards establishing small-to-full scale correlating techniques on jet flap V/STOL aircraft configurations. Lift and drag coefficients from the model and aircraft tests were found to be in reasonable agreement. The pitching moment coefficient and trim condition correlation was poor.

A secondary objective was to evaluate a modified thrust nozzle having thrust reversal capability. The results showed there was a considerable loss of lift in the reverse thrust operational mode because of increased nozzle-wing flow interference.

A comparison between the model simulated H.126 wing jet efflux and the model uniform pressure distribution wing jet efflux indicated, generally, no more than 5% loss in weight flow rate.

17. Key Words (Suggested by Author(s))	18. Distribution Statement
STOL Jet flap	Unclassified - Unlimited STAR Category - 05

19. Security Classif. (of this report)	20. Security Classif. (of this page)	21. No. of Pages	22. Price*
Unclassified	Unclassified	42	$ 3.75

*For sale by the National Technical Information Service, Springfield, Virginia 22151

NOTATION

A	nozzle exit area, sq m (sq ft)
b	wing span, m (ft)
$\bar{c}$	wing mean aerodynamic chord, m (ft)
C_D	drag coefficient, drag/qS
C_J	jet momentum coefficient, F/qS
C_L	lift coefficient, lift/qS
C_m	pitching moment coefficient, pitching moment/$qS\bar{c}$
C_p	pressure coefficient, $(P - P_o)/q$
D	drag, N (lb)
F	jet momentum force, N (lb)
L	lift, N (lb)
P	pressure, absolute, N/sq m (lb/sq ft)
q	freestream dynamic pressure, N/sq m (lb/sq ft)
S	wing area, sq m (sq ft)
T_s	stagnation temperature, °K (°R)
w	air weight flow rate, N/sec (lb/sec)
Y	side force, N (lb)
α	model horizontal datum angle of attack, deg
α_w	wing angle of attack, deg
δ_f	flap/aileron deflection angle, deg
η_T	tailplane angle relative to horizontal datum, deg

Subscripts

AC	air chamber
AMB	ambient

Subscripts (Cont.)

N	fuselage nozzle
PJ	pitch jet
o	free stream
ST	stagnation
w	wing

LOW SPEED WIND TUNNEL TESTS ON A ONE-SEVENTH SCALE MODEL OF THE H.126 JET FLAP AIRCRAFT

Georgene H. Laub

SUMMARY

Low speed wind tunnel tests were performed on a one-seventh scale model of the British H.126 jet flap research aircraft over a range of jet momentum coefficients.

The primary objective was to compare model aerodynamic characteristics with those of the aircraft, with the intent to provide preliminary data needed towards establishing small-to-full scale correlating techniques on jet flap V/STOL aircraft configurations. Lift and drag coefficients from the model and aircraft tests were found to be in reasonable agreement. The pitching moment coefficient and trim condition correlation was poor.

A secondary objective was to evaluate a modified thrust nozzle having thrust reversal capability. The results showed there was a considerable loss of lift in the reverse thrust operational mode because of increased nozzle-wing flow interference.

A comparison between the model simulated H.126 wing jet efflux and the model uniform pressure distribution wing jet efflux indicated, generally, no more than 5% loss in weight flow rate.

INTRODUCTION

Over a number of years, wind tunnel investigations performed on scale models of conventional type aircraft have reasonably well documented techniques for extending tunnel test results to aircraft flight performance. Flow interference between combinations of wing, rotors, fans, and jets in V/STOL type aircraft configurations, however, can introduce considerable errors in the normal predictive techniques. Comparisons of model and full-scale wind tunnel and flight test data on various V/STOL aircraft are needed to evaluate the significance of scale effects and define the limitations pertinent to V/STOL type configurations.

One such STOL type aircraft is the British H.126 which is a high-wing, flight research vehicle built to investigate the "jet-flap" principle of lift augmentation and propulsion (ref. 1). This aircraft had been tested in the Ames 40x80 Foot Wind Tunnel (refs. 2 and 3), as well as flight tested in the United Kingdom,

(data unpublished). With full-scale test data available for correlation, a one-seventh scale model of the H.126 aircraft was constructed and tested in the AAMRDL 7x10 Foot Wind Tunnel.

Two additional objectives were incorporated in the test program: (1) to evaluate the performance of a modified thrust nozzle configuration having thrust reversal capability, and (2) to compare the efficiency of the wing jet efflux of the flight vehicle with that of a uniform pressure distribution wing jet efflux.

MODEL AND APPARATUS

A photograph of the model mounted in the 7x10 Foot Wind Tunnel is shown in figure 1. Pertinent dimensions and geometric data for the model and the modified nozzle are presented in figures 2 and 3, respectively. The model center of rotation (fig. 2(a)) was positioned on the centerline of the tunnel test section. The addition of a fairing over the model engine intake and the absence of intake flow were the only deviations from the aircraft configuration tested in the 40x80 Foot Wind Tunnel.

The model incorporated a full-span wing jet flap, fuselage thrust nozzles, and pitch control jets. Installed within each wing were eight sets of "fish-tail" nozzles patterned to give a wing jet exit pressure distribution representative of the flight vehicle. A plan view of these "fish-tail" nozzle configurations in the wing is shown in figure 4. Air for the port and starboard wing jets was supplied through individual channels in the model mounting strut. Tubing, located fore and aft of the mounting strut, supplied air for the fuselage thrust nozzles and the pitch control jet nozzle. Through each of these four air supply lines, flow rates were regulated by a remotely-located valve and measured by an orifice type flow meter. Two valves, located in the model, controlled the flow to the port and starboard fuselage thrust nozzles.

The model's flap and aileron were constructed as a single piece and flap/aileron deflections were set using fixed-angle brackets. The rudder and elevator, being integral with the fin and tailplane, were fixed at zero degrees deflection. Model tailplane incidence was set at an angle of 4° to correspond to the condition of zero elevator deflection on the aircraft in the 40x80 tunnel test configuration. Model angle of attack, referenced to aircraft horizontal datum, was remotely-controlled.

Twenty-nine pressure orifices were located at each of four spanwise stations normal to leading edge in the port wing, (see fig. 2(b)). Pressures were measured at any pair of inner and outer stations during a single run.

The two fuselage locations for the modified thrust nozzles (fig. 3) are shown in figure 2(a). The change from the thrust mode to the reverse thrust mode was made by interchanging the port and starboard nozzle; i.e., a 180° rotation in the horizontal plane.

TESTS AND PROCEDURES

Forces from each of the model blowing systems were individually controlled to approximate the momentum force relationship existing between the various systems on the aircraft. This relationship, as determined from the aircraft tunnel tests (ref. 2) indicated the fuselage nozzle force to be approximately 60% of the wing jet force and the pitch jet force (for 4 degrees of tailplane incidence) approximately 8% of wing jet force. Measured forces from each of the jet blowing systems, calibrated during wind-off tests, are presented in figure 5 for the basic model, and in figure 6 for the modified nozzles. Calculated jet momentum forces, based on flow rates obtained from pressure and temperature measurements at the flange-tap orifice flow meters, are also included in these figures. The calculated and measured values agree fairly well with the exception of those on the modified nozzle in the reverse thrust mode (fig. 6(b)). This mode required higher operating pressures than the thrust mode for the same flow rate. The slope of a line through the measured data would approximate that for sonic flow conditions; this suggests the possibility that sonic velocities were attained and would account for the higher losses.

In general, the tests were conducted at a nominal tunnel dynamic pressure of 406 N/m^2 (8.5 psf) for a range of wing jet momentum coefficients from 0.08 to 0.9. During any one test, model flap/aileron deflection was set at either 30 or 40 degrees, jet momentum coefficient held constant, and angle-of-attack varied. Tests evaluating the modified thrust nozzle in the thrust and reverse thrust mode were made with the nozzle at two fuselage locations and the flap/aileron deflection set at 40°. Tests comparing wing jet exit pressure distributions were made at a dynamic pressure of 0 and 1197 N/m^2 (0 and 25 psf) for flap/aileron deflections of 0 and 40 degrees and wing air chamber pressure was varied.

Measured aerodynamic forces were resolved with respect to wind axes; aerodynamic moments, referenced to 40% mean aerodynamic chord on the horizontal datum (fig. 2a)), were resolved with respect to stability axes. Due to uncertainties involved in the determination of wind-tunnel wall effects for models of this type, the data are presented without wind-tunnel wall corrections.

RESULTS AND DISCUSSION

Basic Model - Model lift, drag, and pitching moment coefficients at various jet blowing conditions are presented in figures 7 and 8 for flap/aileron deflections of 30 and 40 degrees, respectively. The blowing parameters on the model did not adequately duplicate those of the aircraft and the full-scale and model test results are not compared in this form. The model aerodynamic characteristics for wing jet blowing only are shown plotted at two values of dynamic pressures as a function of wing jet momentum coefficient in figure 9; the general agreement of this data indicates negligible Reynolds number effects at conditions from 1/7 to 1/4 of the full-scale Reynolds number. Lift, drag and pitching moment coefficients from the aircraft tunnel tests (ref. 2) and lift coefficients from flight tests (ref. 4, fig. 7) are compared with adjusted model data at angles of attack of 0 and 8 degrees in figures 10(a) and 10(b), respectively.

Linear corrections, adjusting for model deviations from the aircraft fuselage and pitch jet blowing relationship, have been made to the model test results presented in this figure. Also included in figure 10(a) are the data from figure 9 which required the maximum correction to include the effect of fuselage and pitch jet blowing. The good agreement of the partially and fully adjusted model aerodynamic coefficients indicates no significant interaction effects between the model blowing systems and tends to substantiate this means of model data correction. Aircraft and model lift and drag coefficients compare reasonably well at the conditions shown. Comparison of full-scale and model pitching moment coefficients, however, show discrepancies as large as 0.3 over the operational wing jet momentum coefficient range. This difference is probably not a result of jet interference effects since it appears to exist at the no blowing condition. Full-scale trim conditions from tunnel tests, RAE flight tests, and BAC flight tests (replotted from ref. 4, figs. 20 and 21) are shown in figure 11 with model trim conditions superimposed. Considering the lack of agreement among full-scale test data, the difference between model and aircraft pitching moment coefficients and trim conditions cannot be attributed to scaling effects without additional evidence. Data were not available to assess the effects of the fairing over the model engine intake and the absence of intake flow.

Chordwise pressure distributions at two spanwise stations with a flap/aileron deflection of 0° and at four spanwise stations with a flap/aileron deflection of 40° are presented in figure 12 for the no jet blowing condition. Data are presented at model angles of attack of ±4 degrees (α_w = 1° and 9°) and although not directly comparable because of three-dimensional effects, calculated two-dimensional pressure distributions for the flap/aileron deflection of 0° are also included. The effect of jet flap blowing on chordwise pressure distributions at model angles of attack of 0 and 8 degrees (α_w = 5° and 13°) and a flap/aileron deflection of 40° can be seen in figure 13(a) and (b). The upper flap surface experienced larger negative pressure coefficients from jet blowing at station 85.68 than at station 24.10, and although not shown, those pressure coefficients at stations 44.62 and 65.30 fell between those at the two outer stations.

Modified Thrust Nozzle. - Model lift, drag, and pitching moment coefficients with the modified thrust nozzle installed at the fore and aft fuselage location (fig. 2) are presented in figures 14 and 15 for a wing jet momentum coefficient of approximately 0.9 and a flap/aileron deflection of 40 degrees. These data are presented for a nominal fuselage thrust to wing jet momentum ratio of 0.6 in the forward and reverse thrust modes and 0.3 in the reverse thrust mode. For comparative purposes, the basic model data without jet blowing are also shown. Operation in the reverse thrust mode had the expected thrust spoiling effect as evidenced in the increased drag coefficient. Interference of the reverse thrust flow from both fuselage locations with flow over the wing resulted in a considerable loss in lift coefficient. This interference can also be seen in the wing pressure distributions presented in figures 16 and 17. With the nozzle at the forward fuselage location, pressures on both surfaces of the inner station, 24.10, show the influence of the reverse thrust flow (fig. 16). With the nozzle at the rearward and higher fuselage station, the reverse thrust flow has the greater influence on the pressures on the upper wing surface at station 24.10. Unless some means can be found to prevent or minimize this flow interference, these lift losses probably negate any further consideration of this nozzle configuration for use on the aircraft.

Wing Jet Efflux Pressure Distributions - Two wing jet exit pressure distributions, one representing the aircraft and the other a uniform exit pressure, have been presented in figure 4. The "fish-tail" nozzle arrangement, constructed to give an exit pressure distribution representing that of the aircraft, has approximately a 97% pressure recovery; however, this is considered high since it is based on the average of pressures measured at the centers of the individual ducts. The configuration without the "fish-tail" nozzles, i.e., the uniform wing exit pressure distribution, has a pressure recovery approaching 99%. Measured flow rates for these two configurations were reduced to the non-dimensional flow parameter, $w\sqrt{T_s}/AP_{AC}$, and the ratio of the two plotted in figure 18 versus the wing air chamber pressure ratio. Data are presented for the port and starboard wing at flap/aileron deflections of 0 and 40° and tunnel dynamic pressures of 0 and 1197 N/m^2 (25 psf). Although the data shows considerable scatter, the flow losses due to the non-uniform pressure distribution appear, generally no greater than 5%.

SUMMARY OF RESULTS

Results of the one-seventh scale H.126 model tests in the 7x10 Foot Wind Tunnel are summarized as follows:

1. Model and aircraft lift and drag coefficients compared reasonably well.

2. Differences in model and full-scale pitching moment coefficients as large as 0.3 existed over the operational jet momentum coefficient range. Since there was considerable variation in trim condition data obtained from aircraft tunnel and flight tests, the differences in model and aircraft pitching moment coefficients and trim conditions cannot be attributed to scaling effects without additional evidence.

3. Flow from the modified thrust nozzle operating in the reverse thrust mode was observed to interfere with the flow over the wing causing a considerable loss of lift.

4. Wing jet weight flow losses of the non-uniform aircraft exit pressure distribution flow pattern, as compared to the uniform exit pressure distribution, appeared, generally, no greater than 5%.

REFERENCES

1. Harris, K. D., The Hunting H.126 Jet-Flap Research, AGARD Lecture Series 43, February 1971.

2. Aiken, Thomas N. and Cook, Anthony M., Results of Full-Scale Wind Tunnel Tests on the H.126 Jet Flap Aircraft, NASA TN-D7252, April 1973.

3. Reed, D. and Leslie, W. D., Aerodynamics Laboratory, Hawker-Siddeley Aviation Limited, Low Speed Wind Tunnel T[illegible] the Hunting H.126 Jet-Flap Aircraft, HSA (Brough), Note No. YWT 1515 L[illegible] ovember 1969.

4. Cowper, J., Aerodynamics Design Department, Hawker-Siddeley Aviation Limited, Report on H.126 Ames Tunnel Tests, HSA (Brough) Note No. YAD 3083, March 1970.

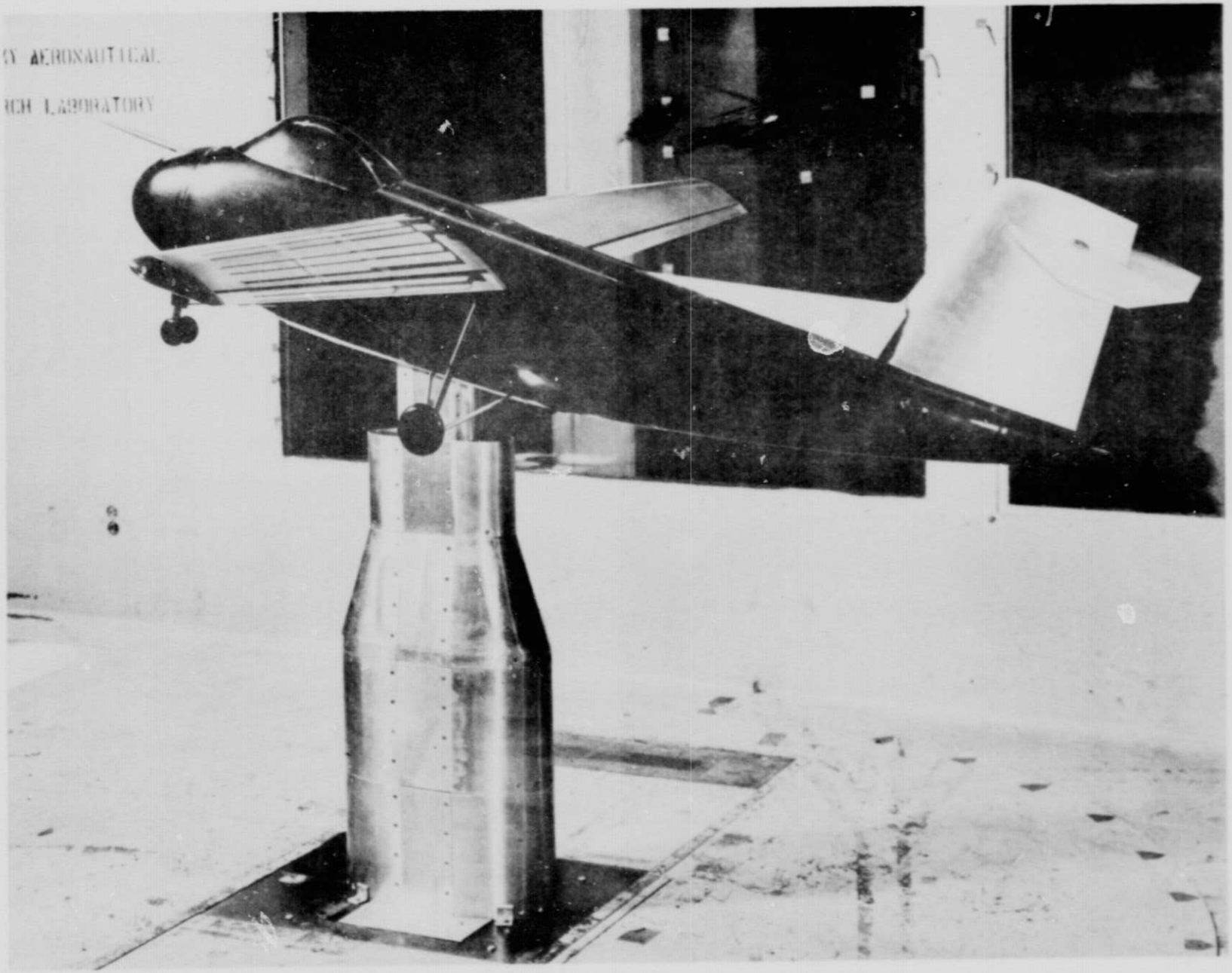

Figure 1. - H.126 Model Installed in the 7x10 Foot #2 Wind Tunnel.

Wing

Airfoil section (Normal to leading edge)	NACA 4424
Area , sq. m.	0.419
Aspect ratio	9.32
Mean aerodynamic chord , cm.	21.98
Span , cm.	197.55
Sweep @ .25 chord , deg.	5.03
Incidence to fuselage datum , deg.	5.00
Root chord , cm.	27.96
Tip chord , cm.	14.42
Taper ratio	0.516

Flap/Aileron

Inboard edge semispan position	0.11
Proportion of semispan	0.84
Root chord , cm.	5.55
Tip chord , cm.	3.17

Horizontal Tail

Airfoil section (Inverted)	NACA 43015
Area , sq. m.	0.104
Aspect ratio	2.55
Span , cm.	51.53
Root chord , cm.	30.30
Tip chord , cm.	10.11
Taper ratio	0.333

Vertical Tail

Airfoil section	NACA 0015
Area , sq. m.	0.100
Aspect ratio	1.18
Height , cm.	34.40
Root chord , cm.	36.29
Tip chord , cm.	22.13

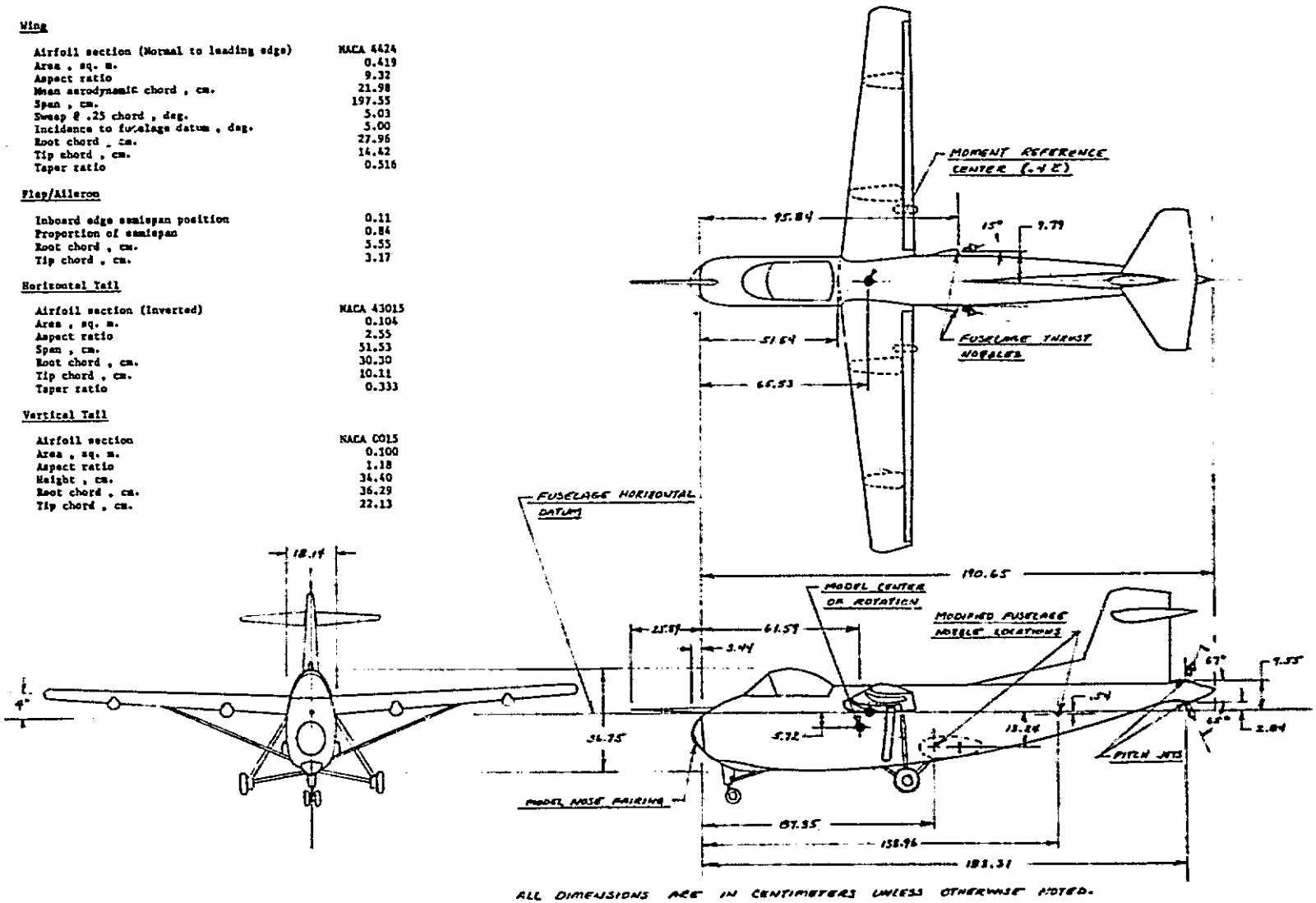

(a) Model Dimensions.

Figure 2. - One-Seventh Scale H.126 Model.

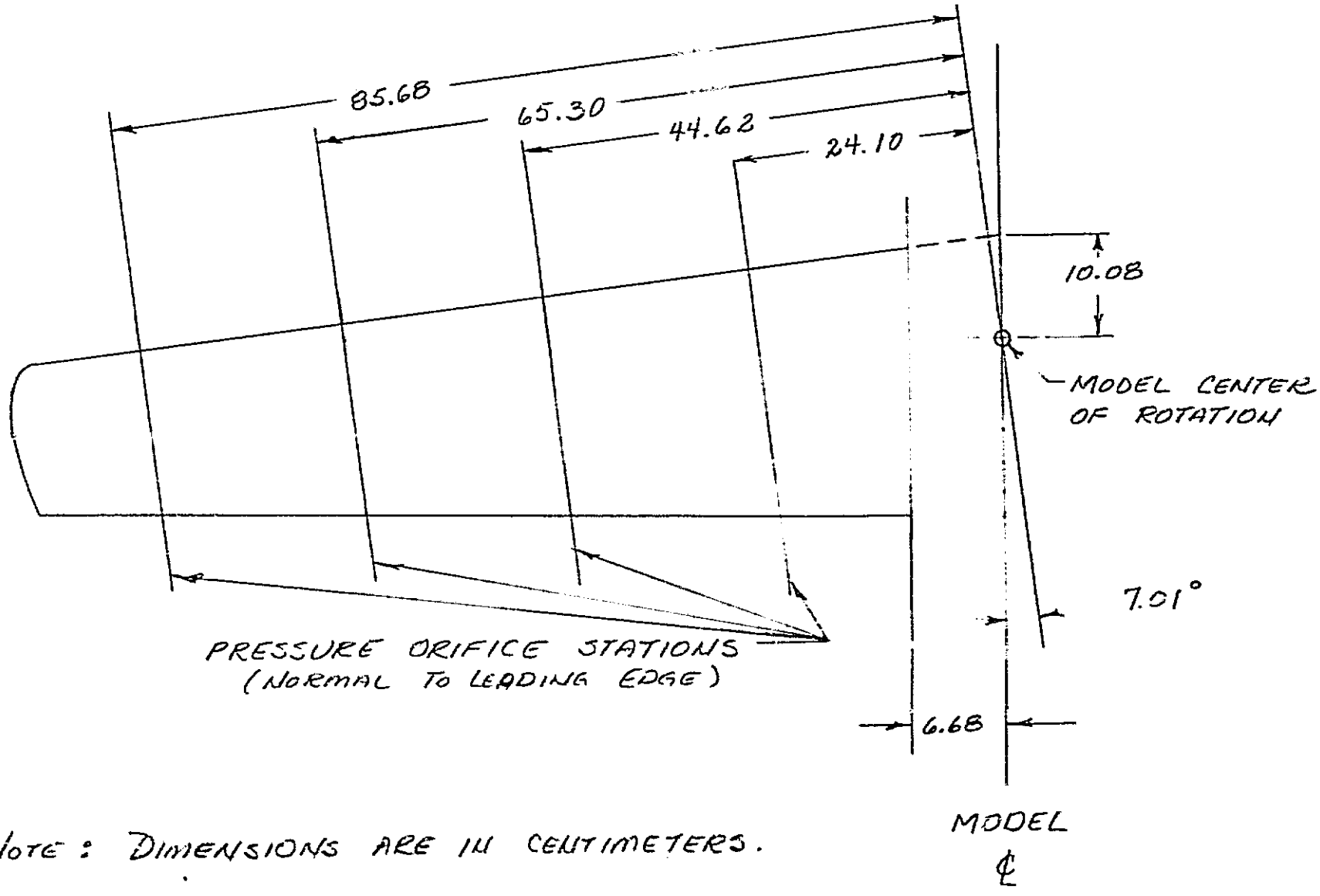

(b) Locations of Pressure Orifice Stations in Plane of Wing Chord.

Figure 2. - Concluded.

Figure 3. - Geometry of Modified Thrust Nozzle.

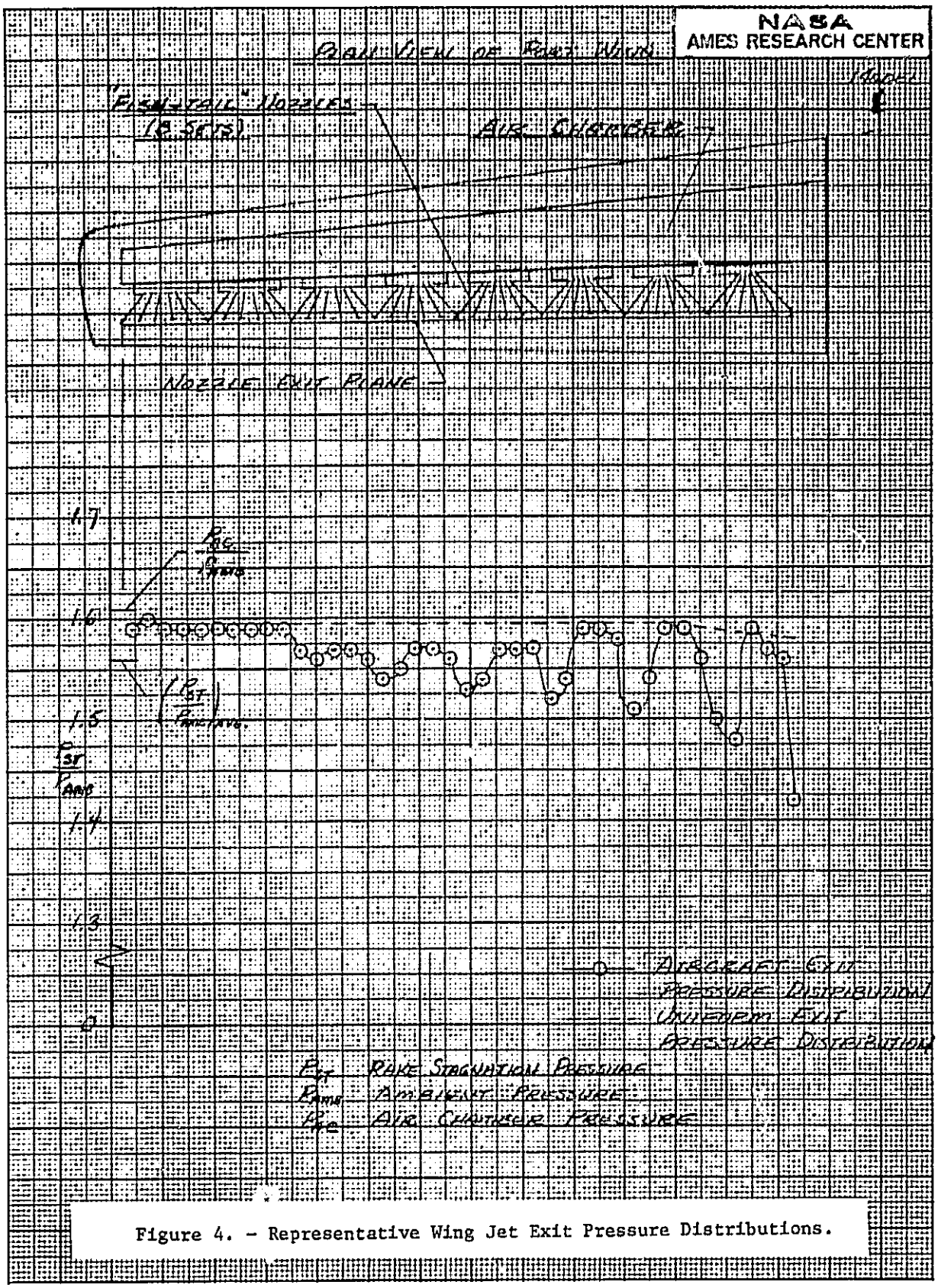

Figure 4. - Representative Wing Jet Exit Pressure Distributions.

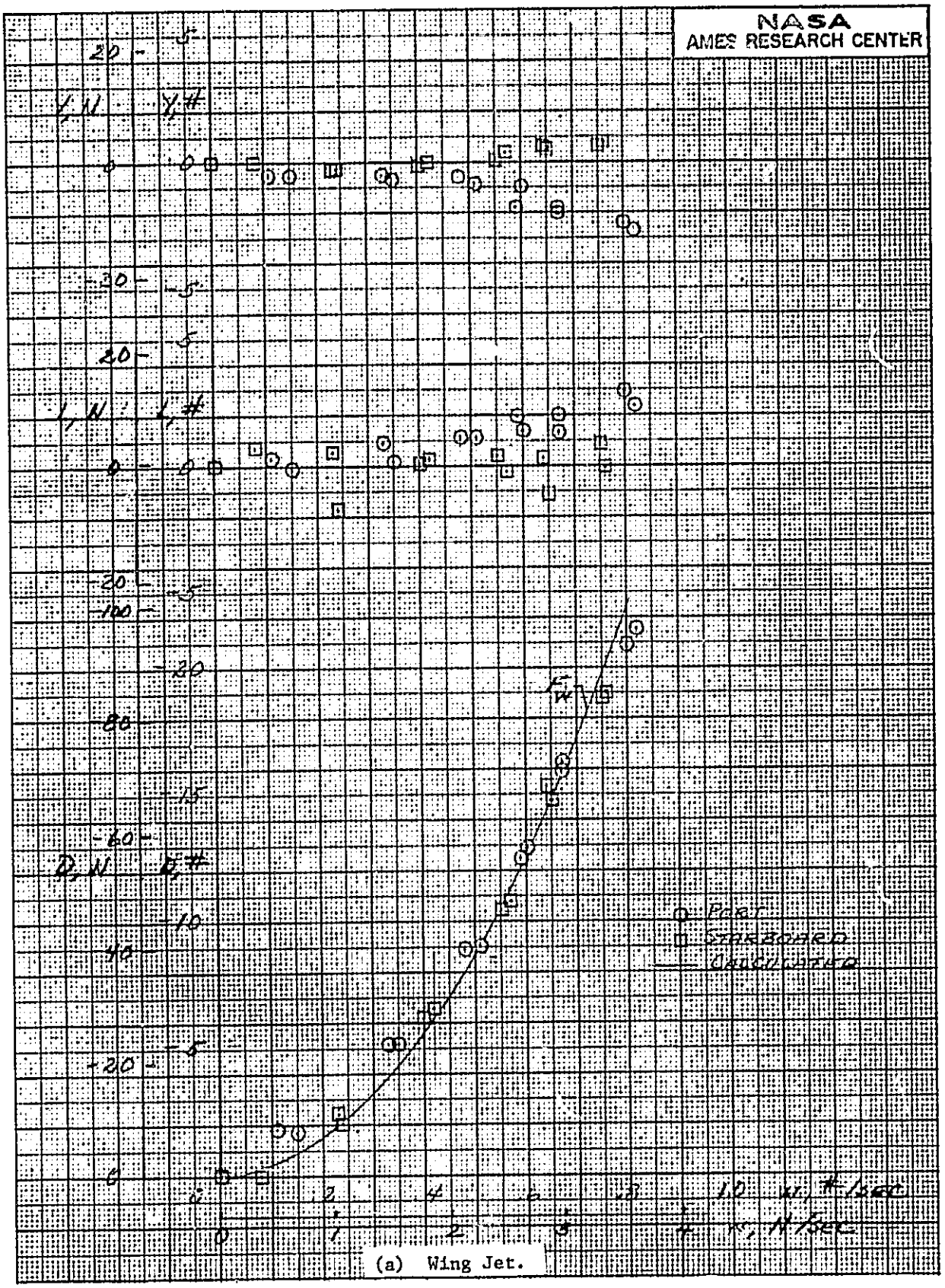

(a) Wing Jet.

Figure 5. - Calibration of Nozzles on Basic Model.

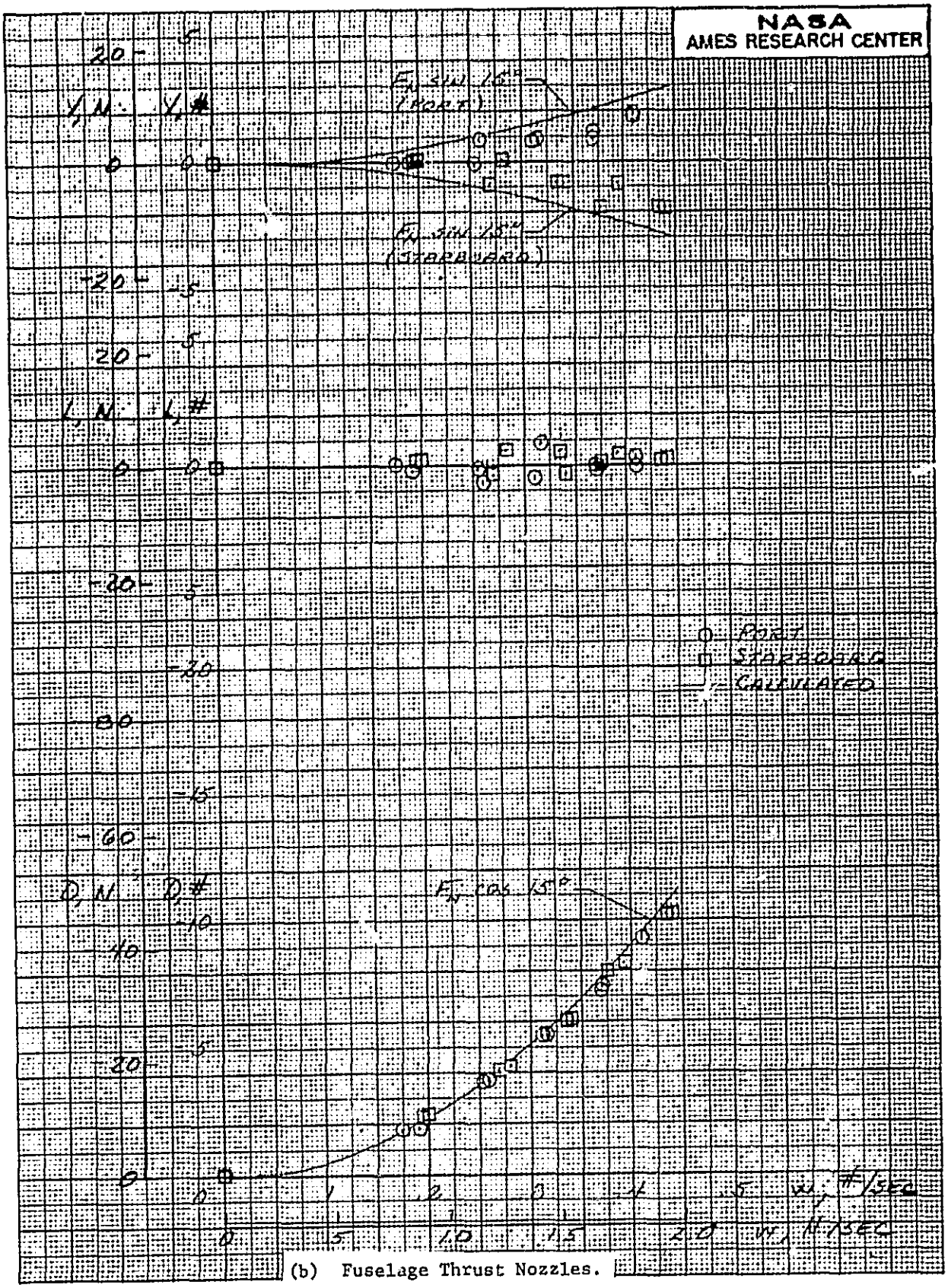

(b) Fuselage Thrust Nozzles.

Figure 5. - Continued.

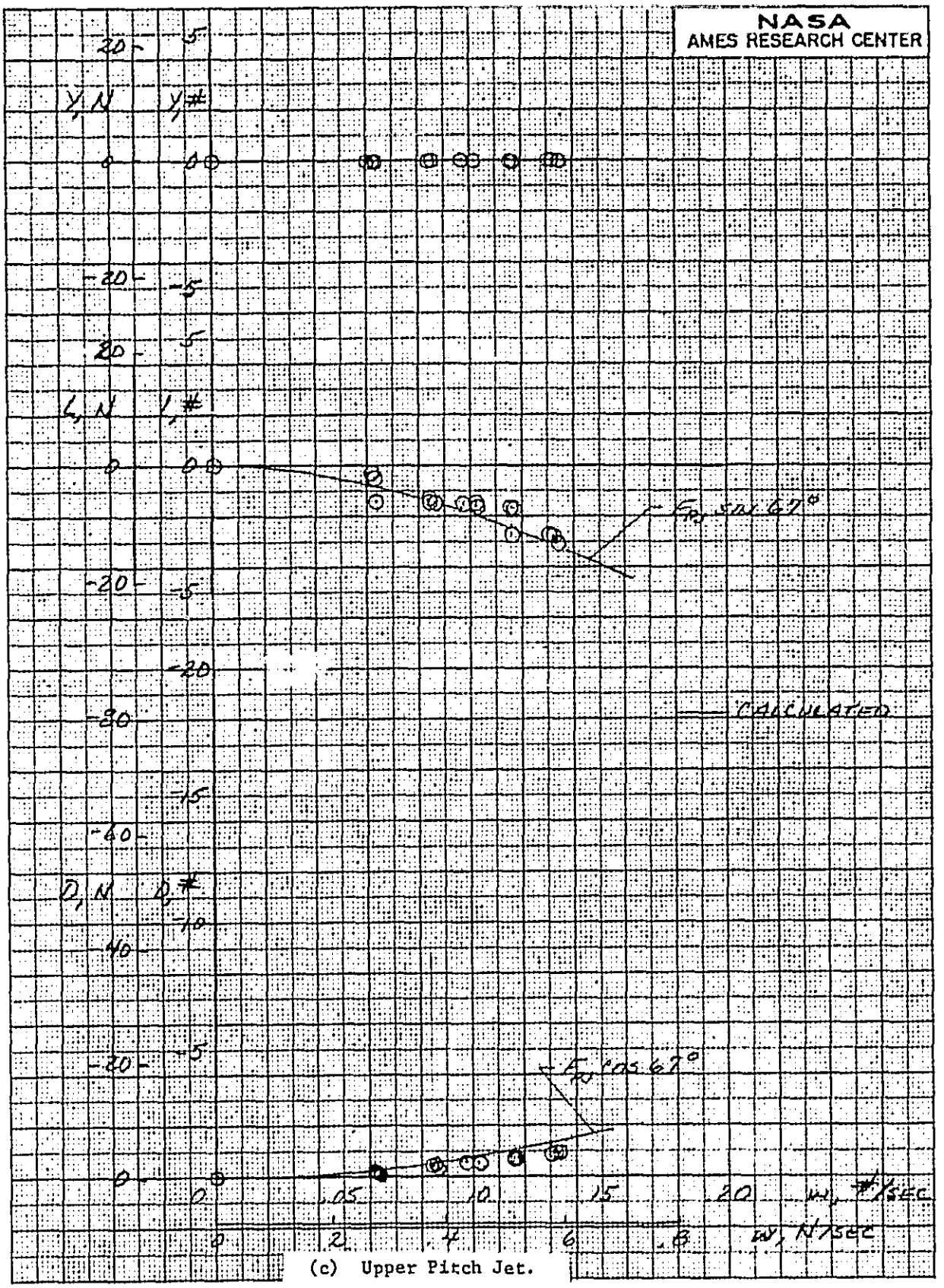

(c) Upper Pitch Jet.

Figure 5. - Concluded.

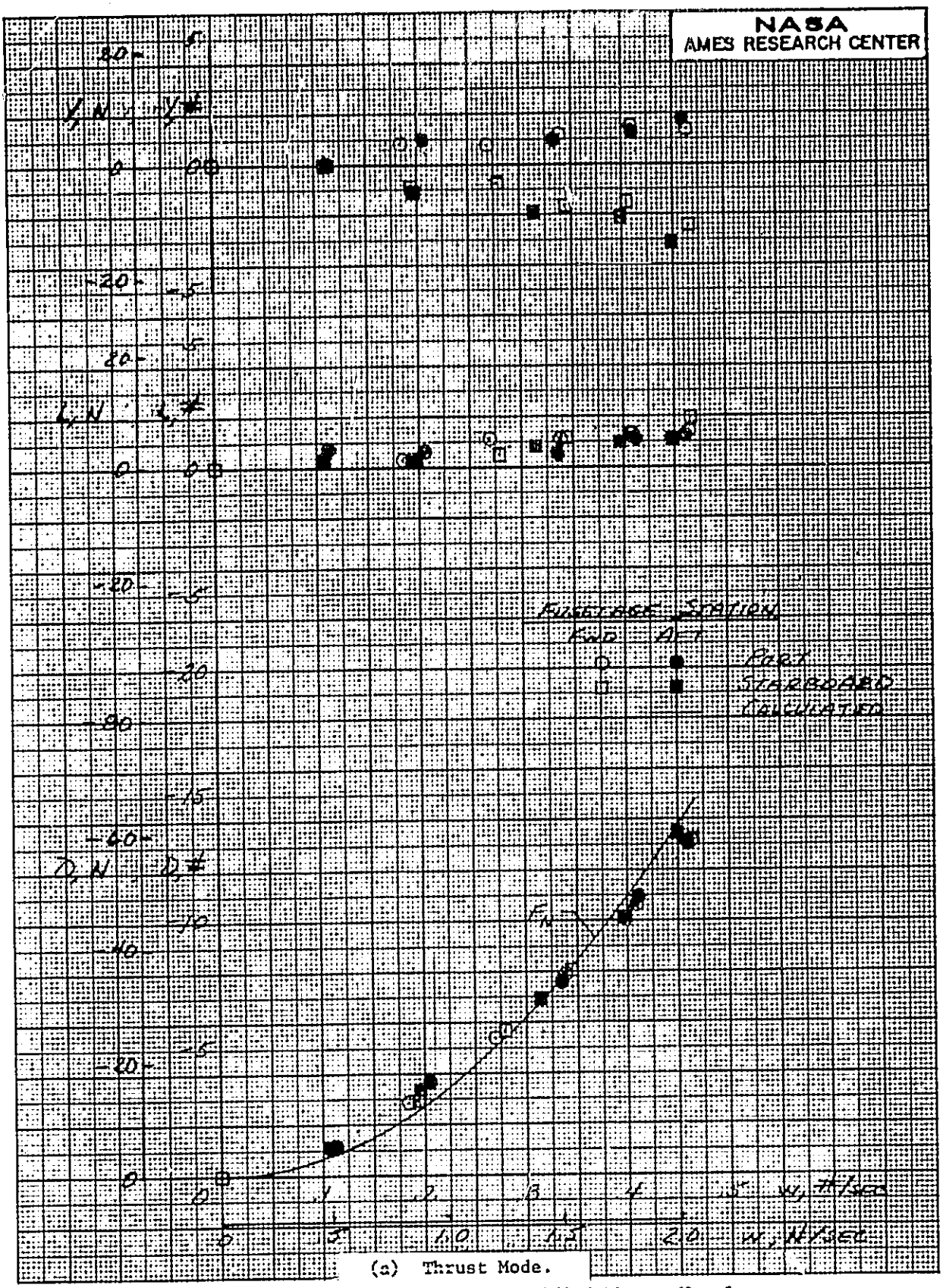

Figure 6. - Calibration of Modified Thrust Nozzles.

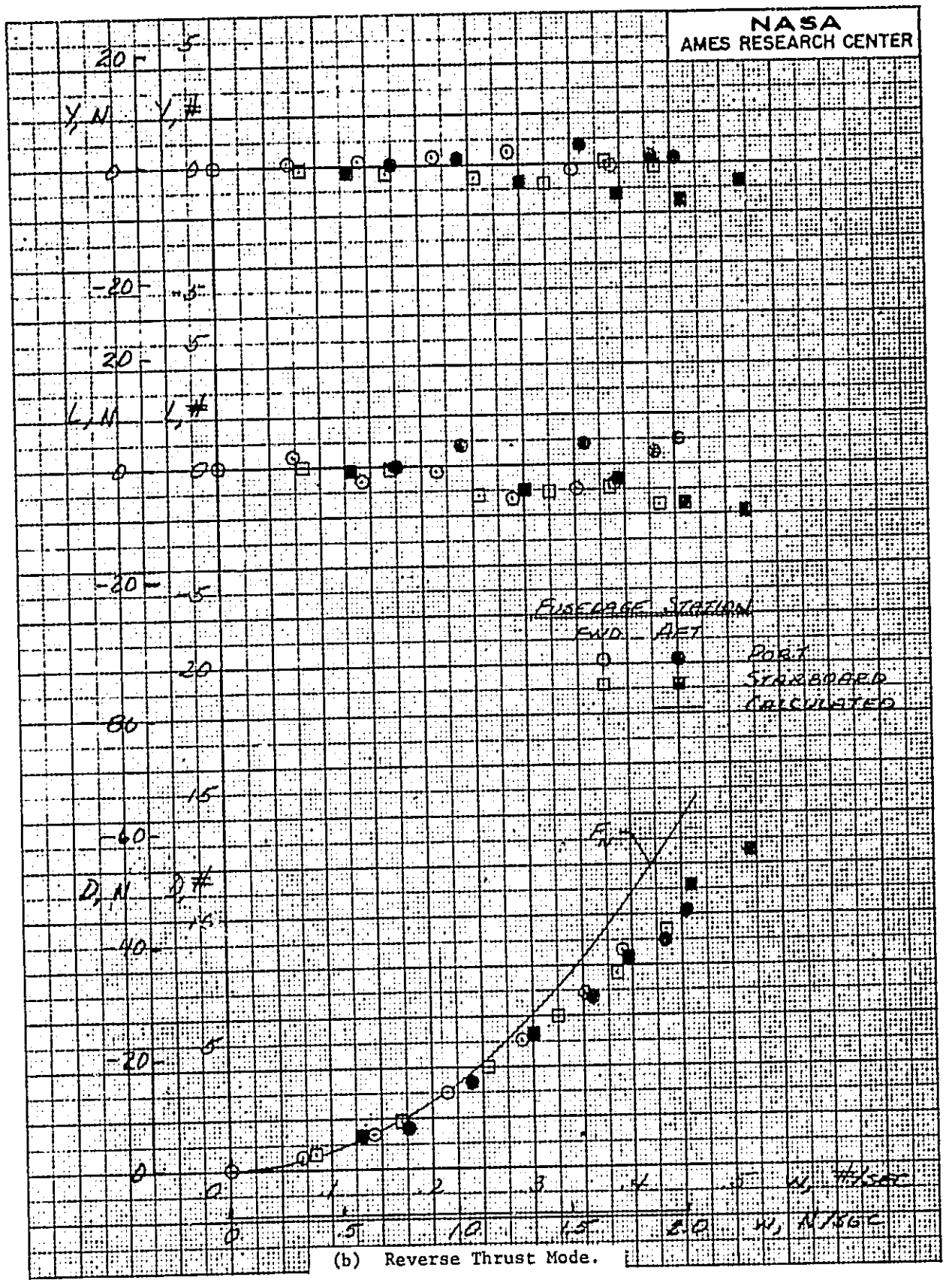

(b) Reverse Thrust Mode.

Figure 6. - Concluded.

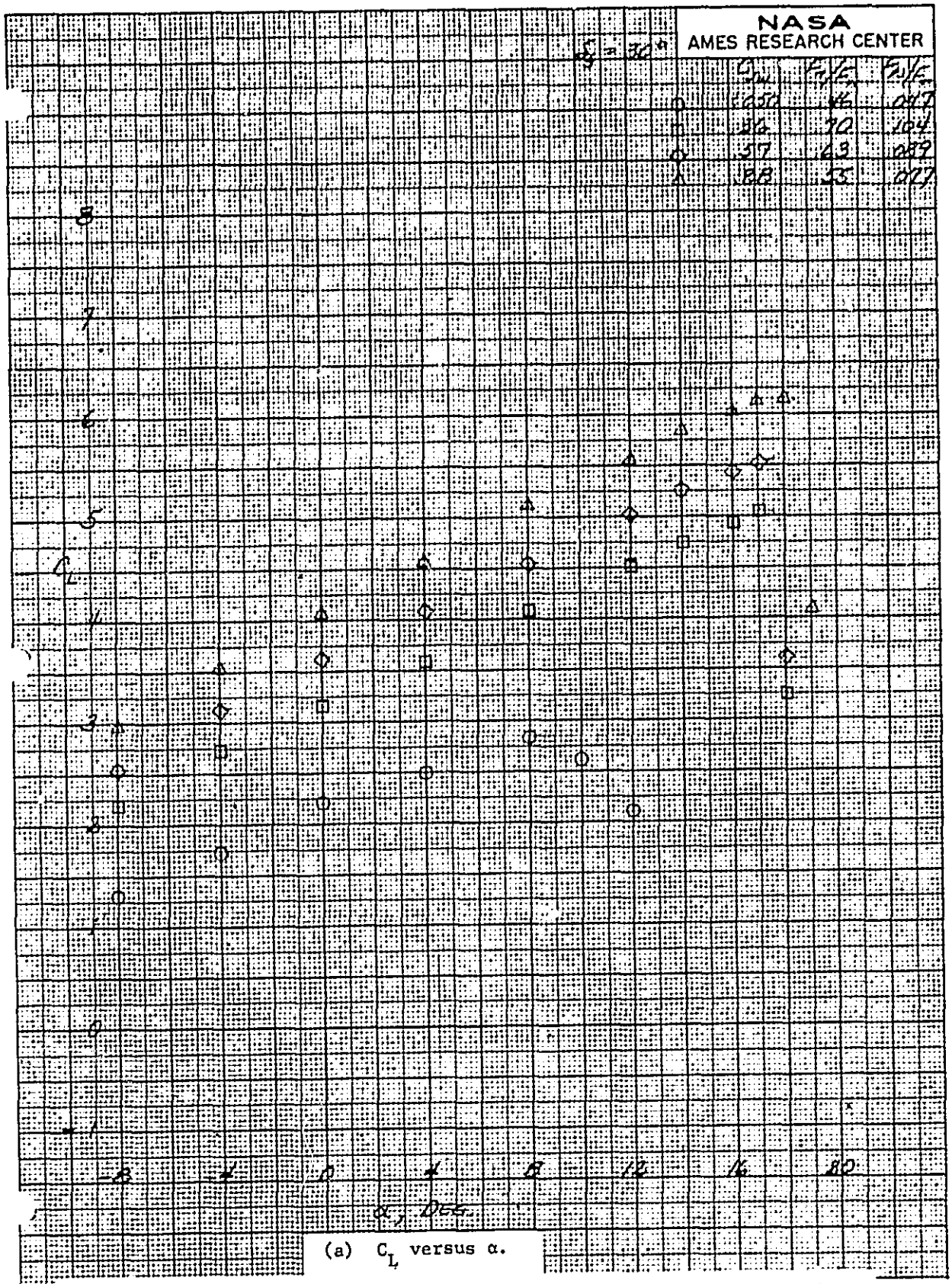

(a) C_L versus α.

Figure 7. – Lift, Drag, and Pitching Moment Coefficients, $\delta_f = 30°$.

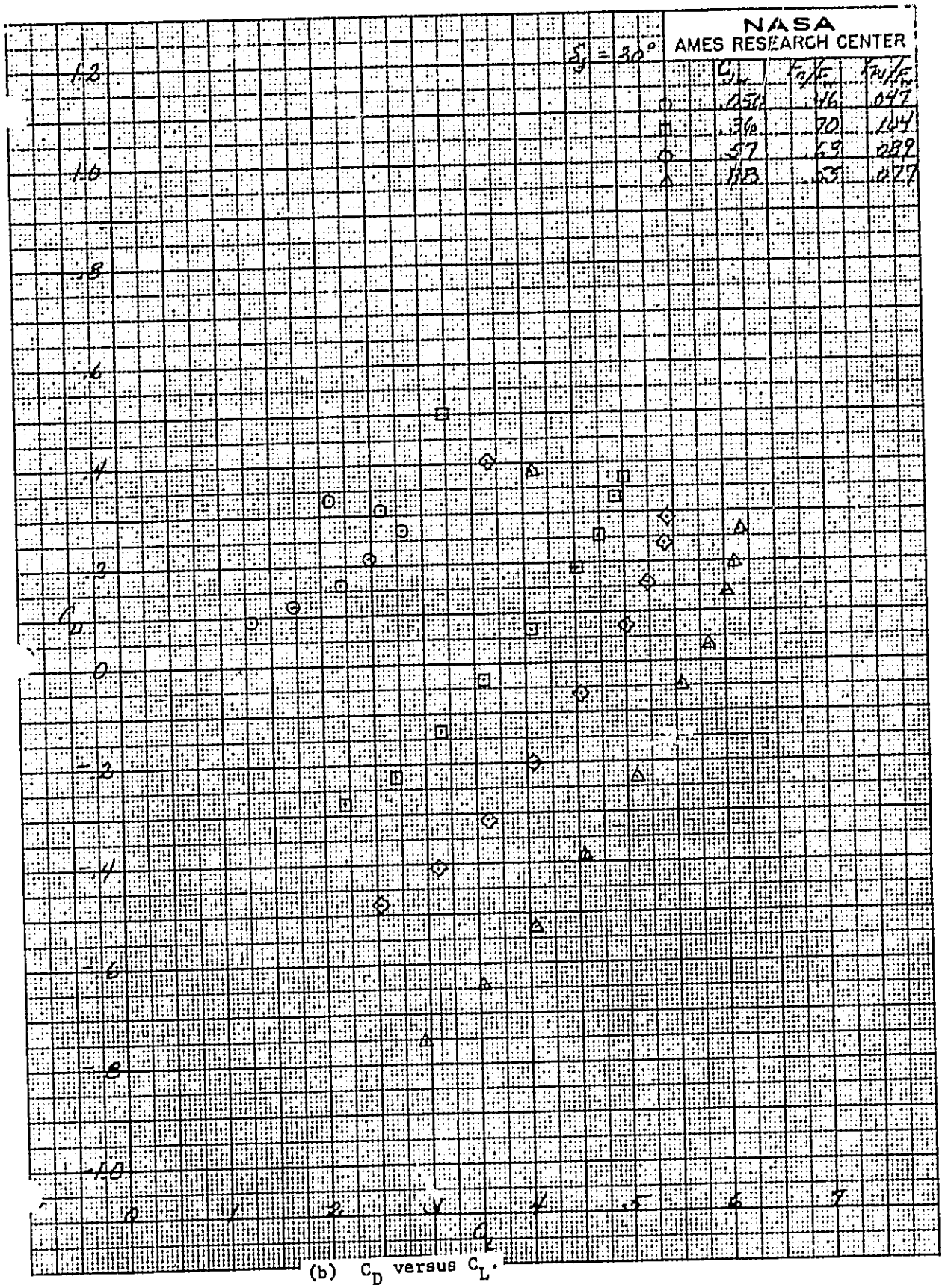

(b) C_D versus C_L.

Figure 7. - Continued.

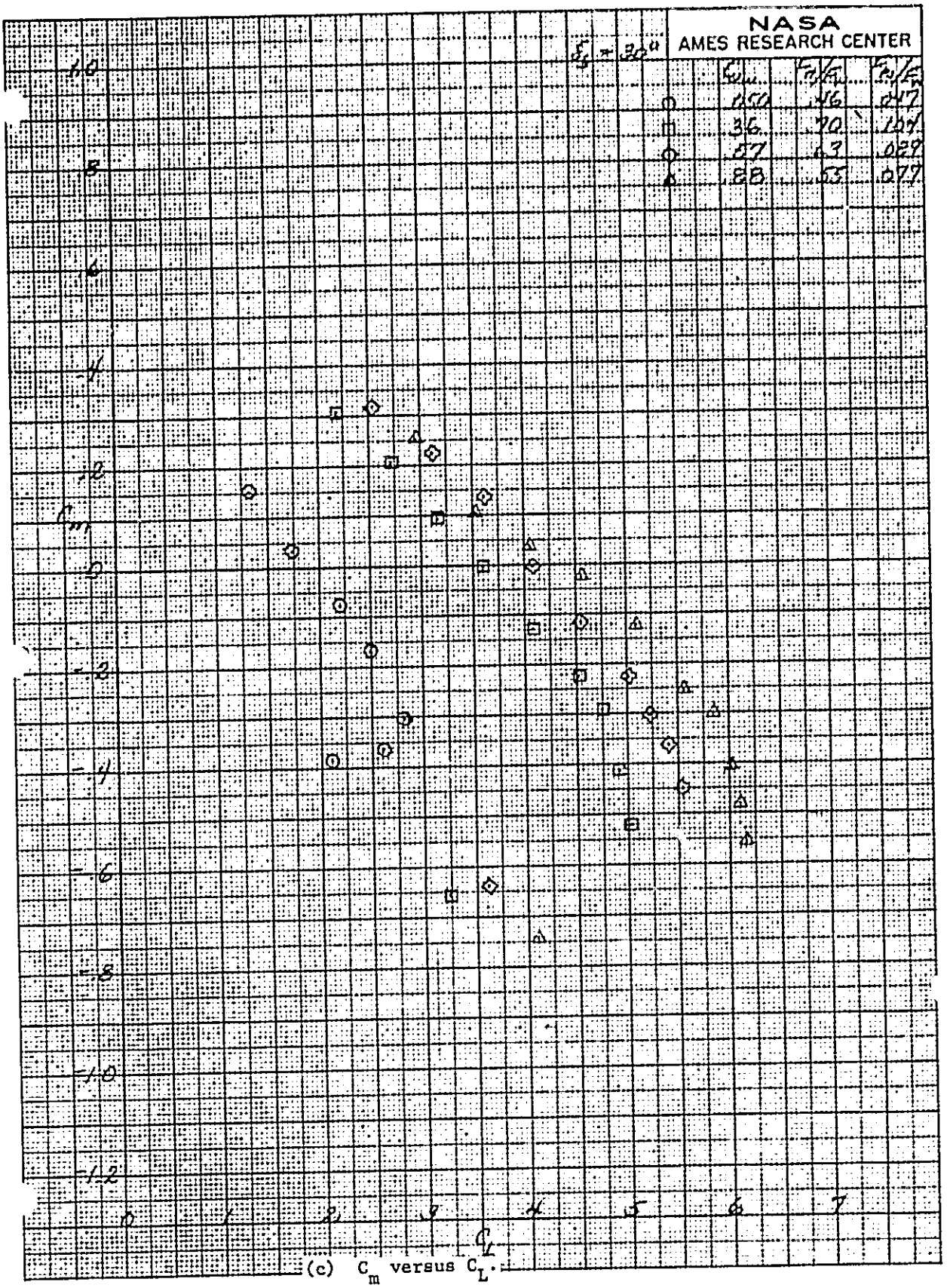

(c) C_m versus C_L.

Figure 7. - Concluded.

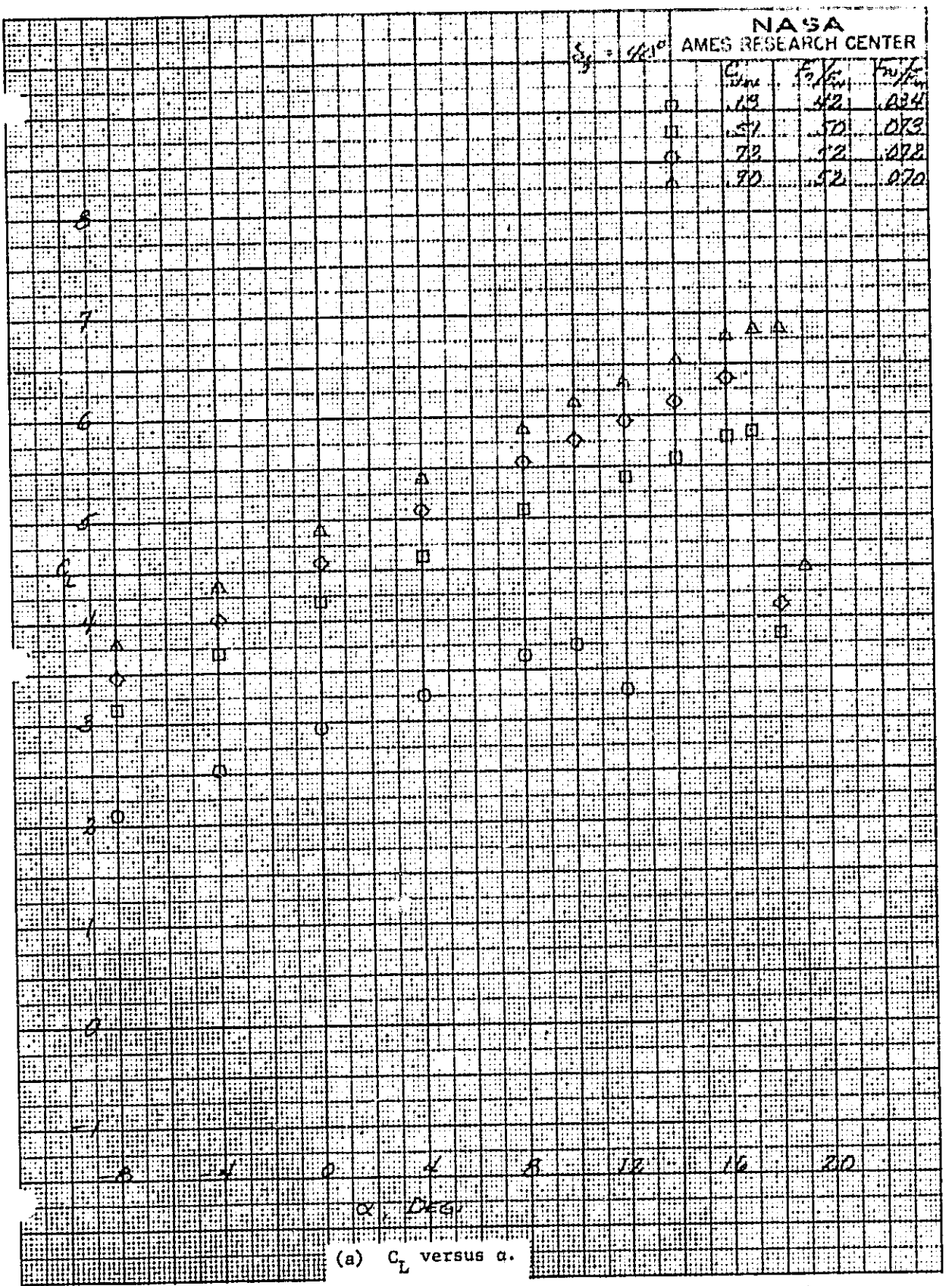

(a) C_L versus α.

Figure 8. - Lift, Drag, and Pitching Moment Coefficients, δ_f = 40°.

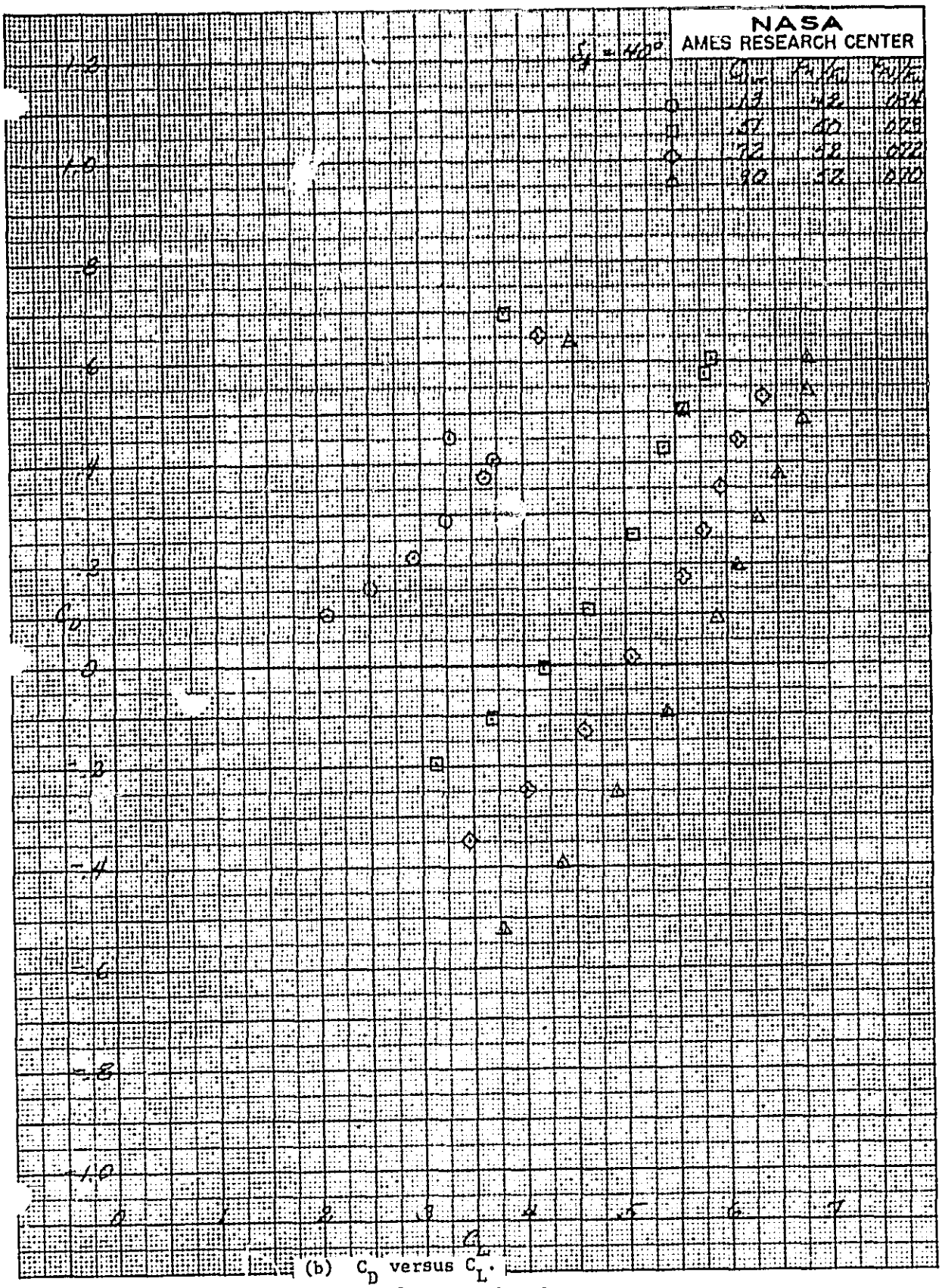

(b) C_D versus C_L.

Figure 8. - Continued.

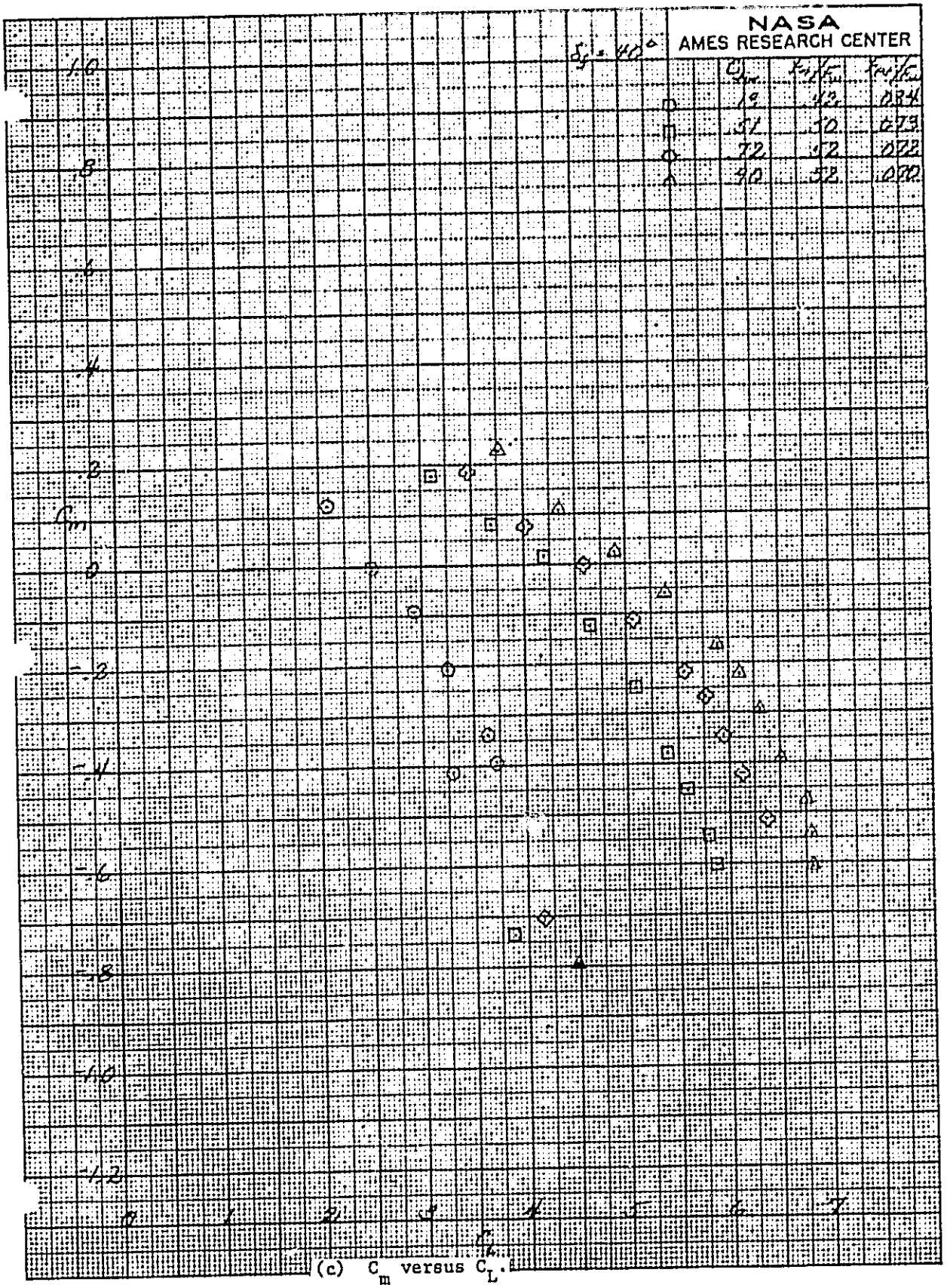

(c) C_m versus C_L.

Figure 8. - Concluded.

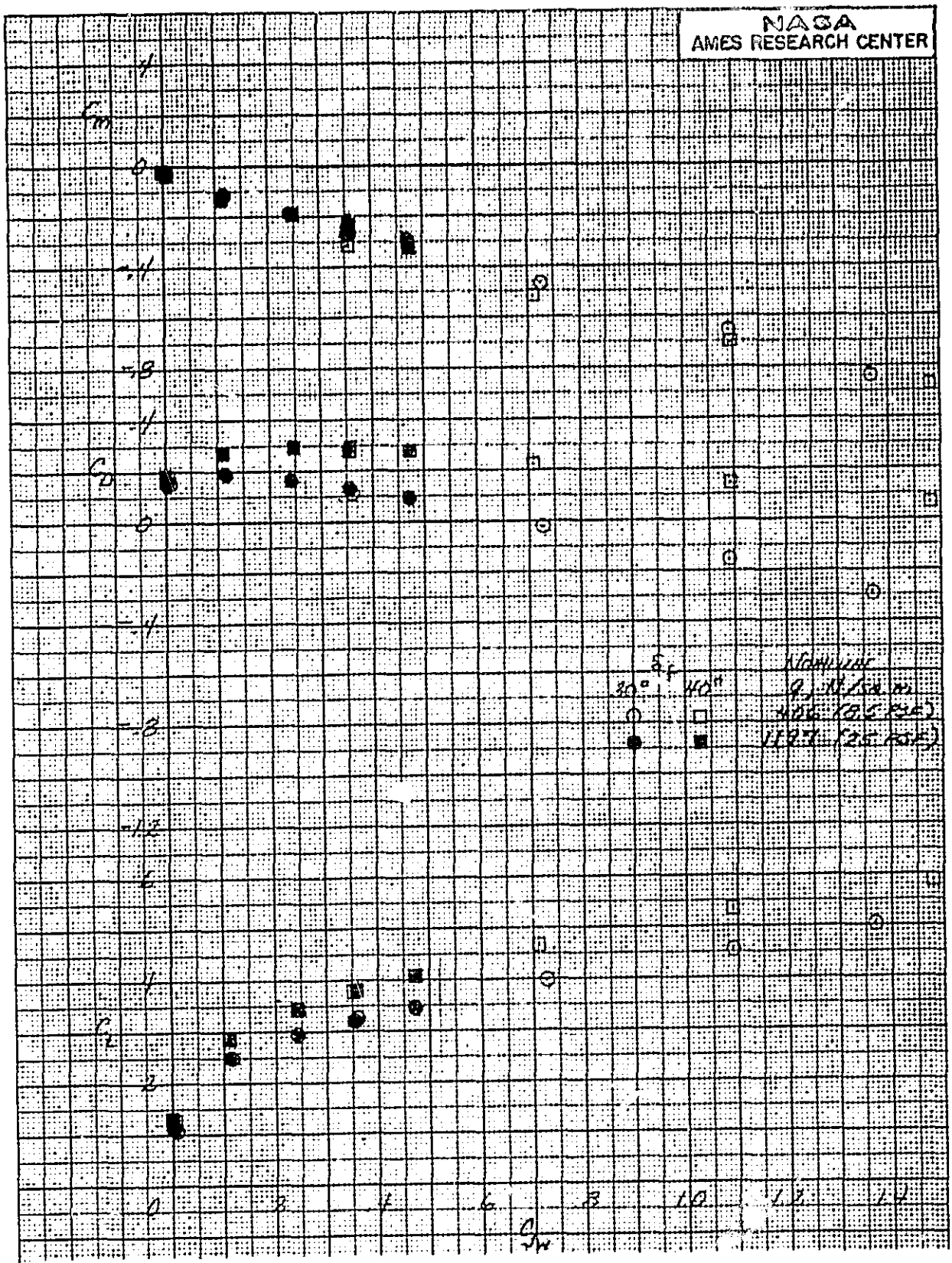

Figure 9. - Effect of Wing Jet Momentum on Model Lift, Drag, and Pitching Moment $F_N/F_w = F_{PJ}/F_w = 0$.

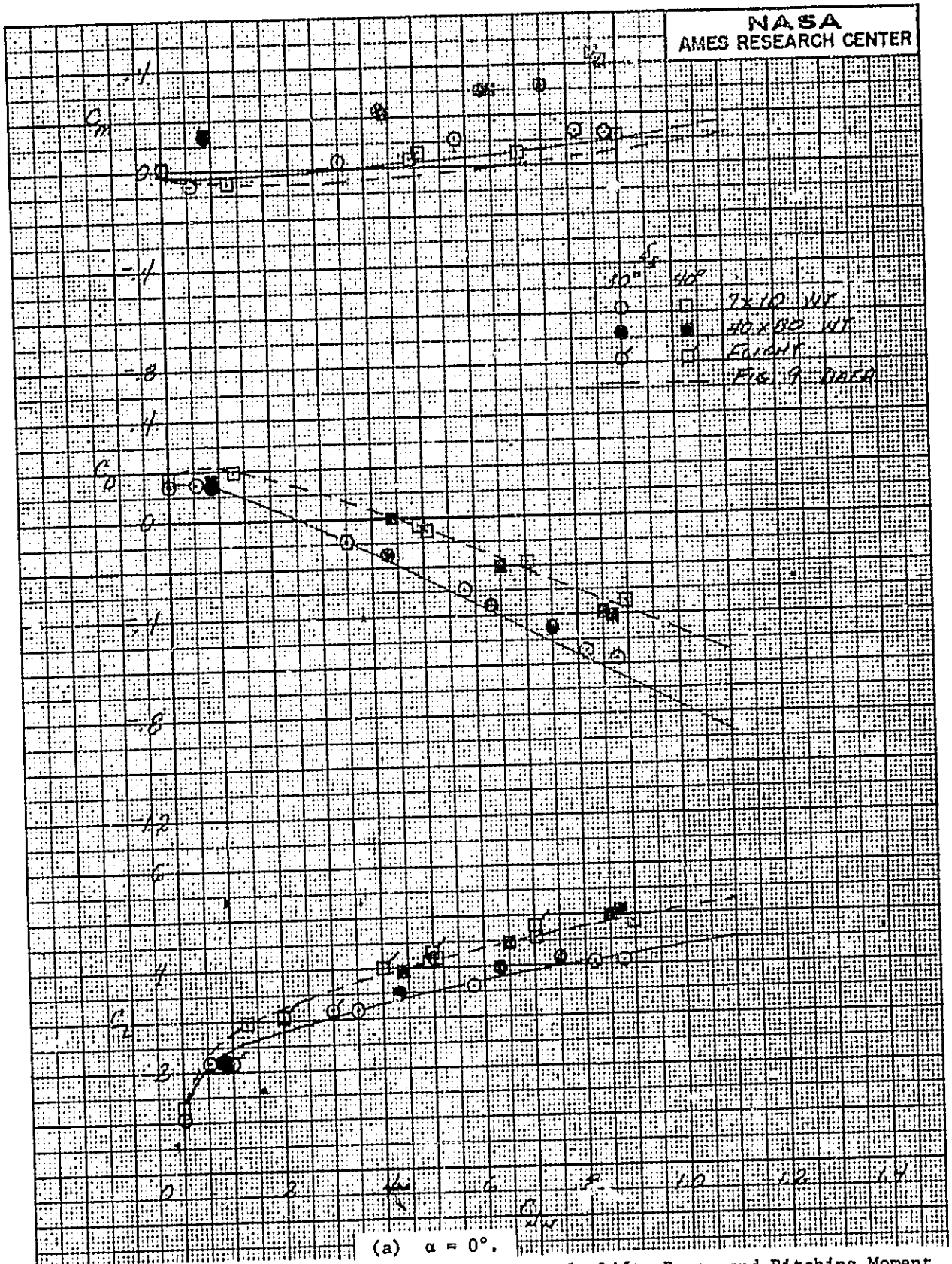

(a) $\alpha = 0°$.

Figure 10. – Comparison of Model and Full-Scale Lift, Drag, and Pitching Moment $F_N/F_w = .6$, $F_{PJ}/F_w = .08$.

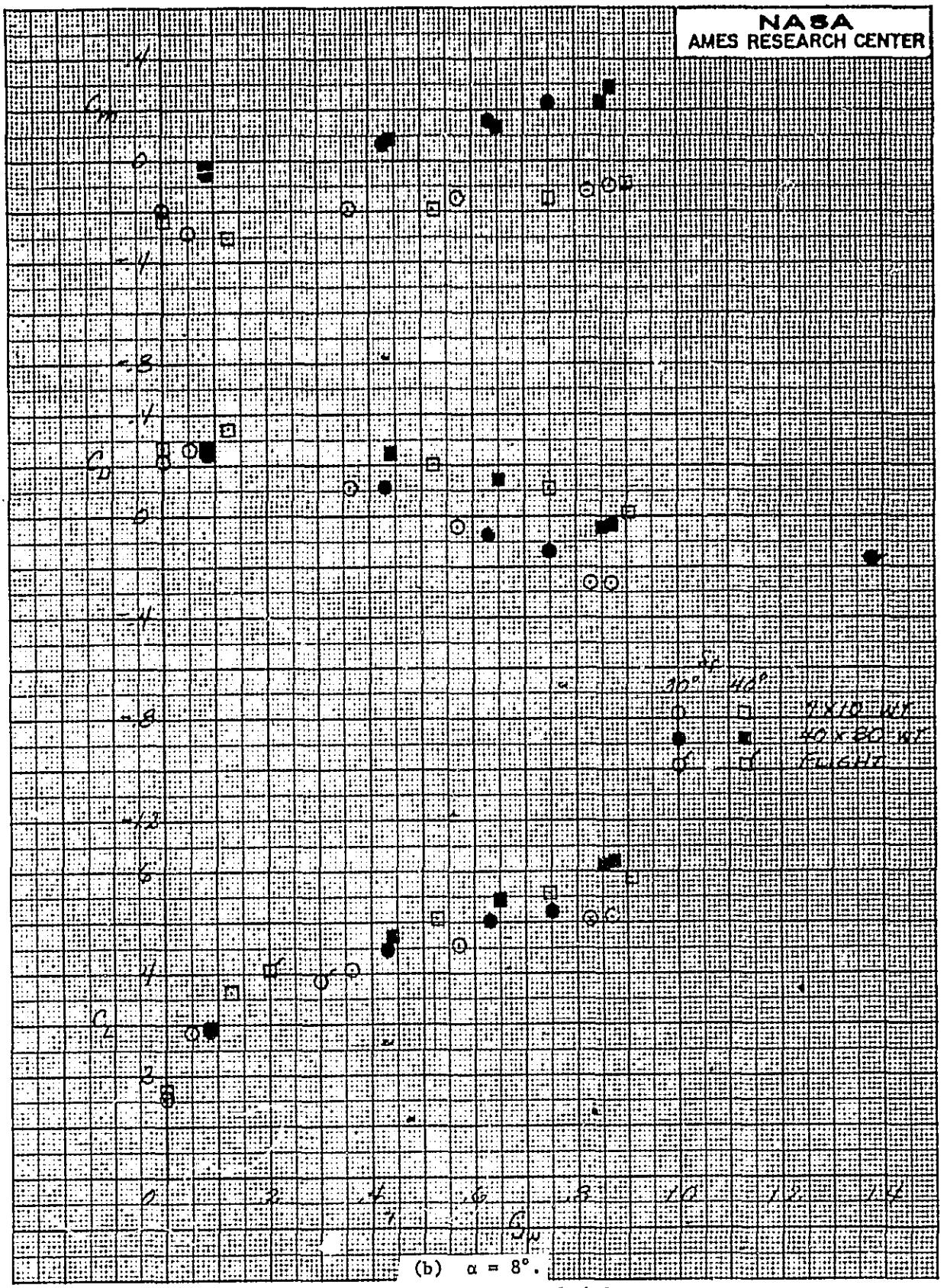

(b) $\alpha = 8°$.

Figure 10. - Concluded.

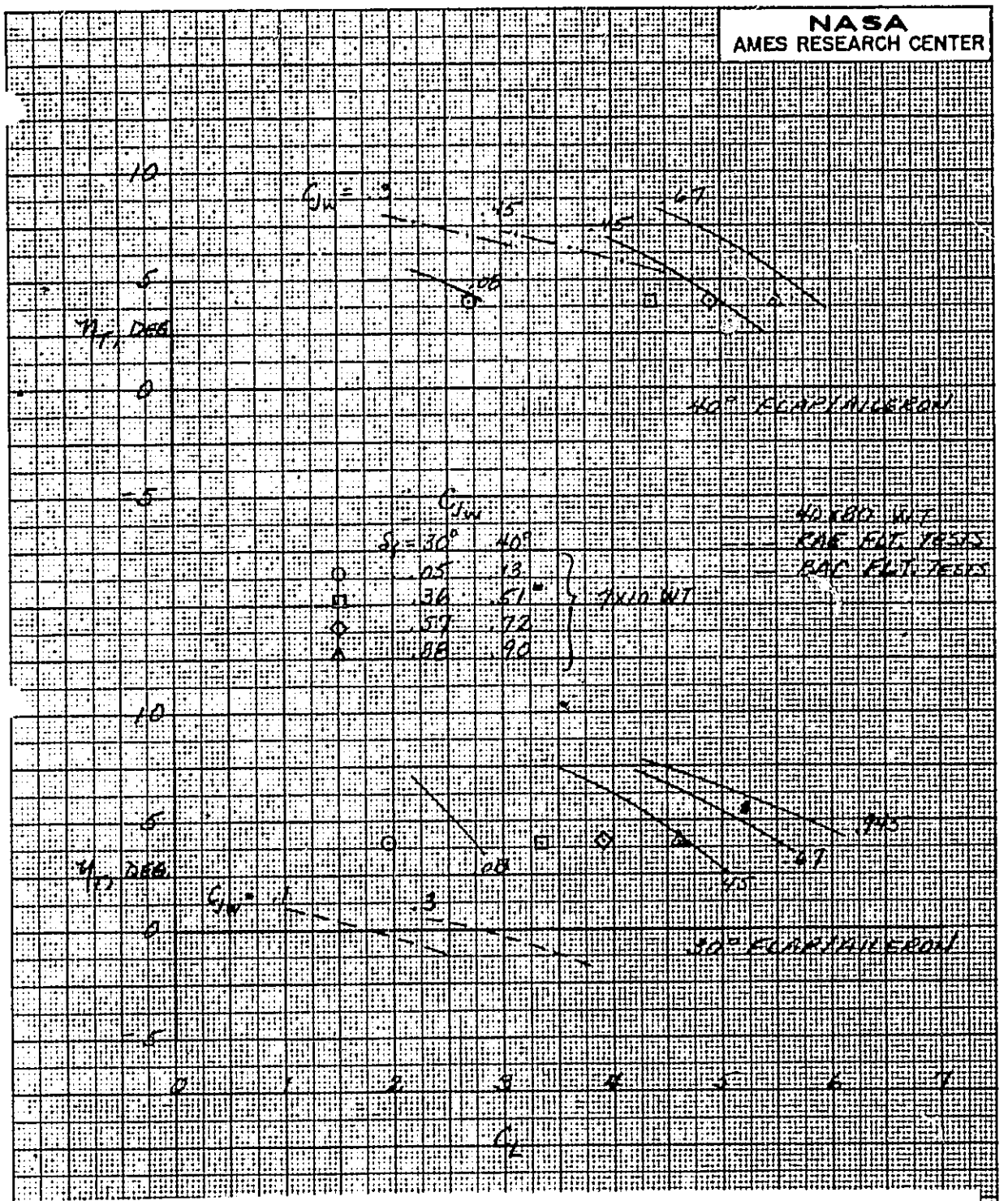

Figure 11. – Model and Full-Scale Tailplane Trim Angle for 0.4 $\bar{c}$ CG Position.

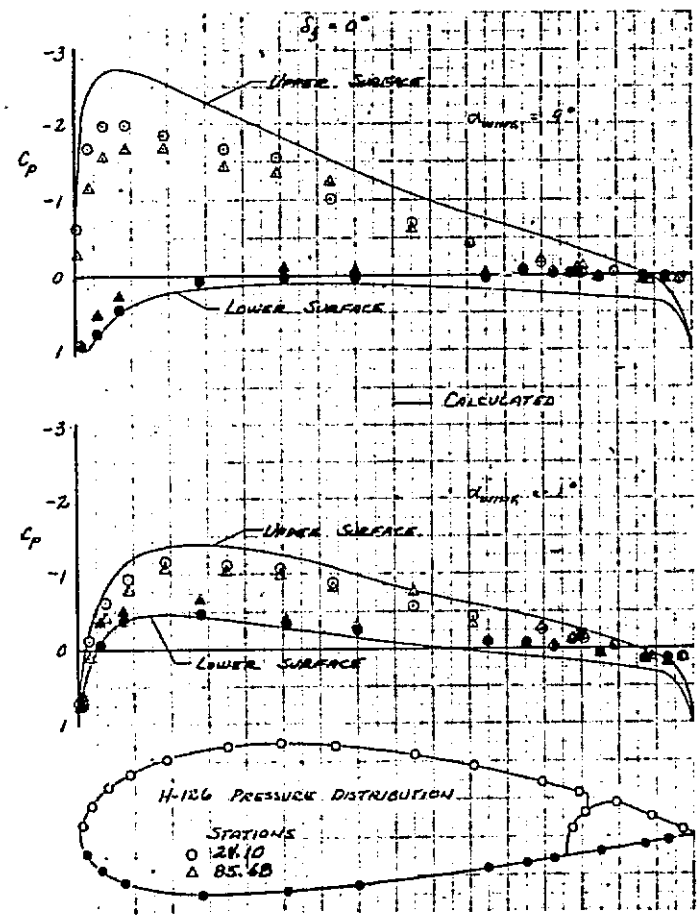

(a) $\delta_f = 0°$.

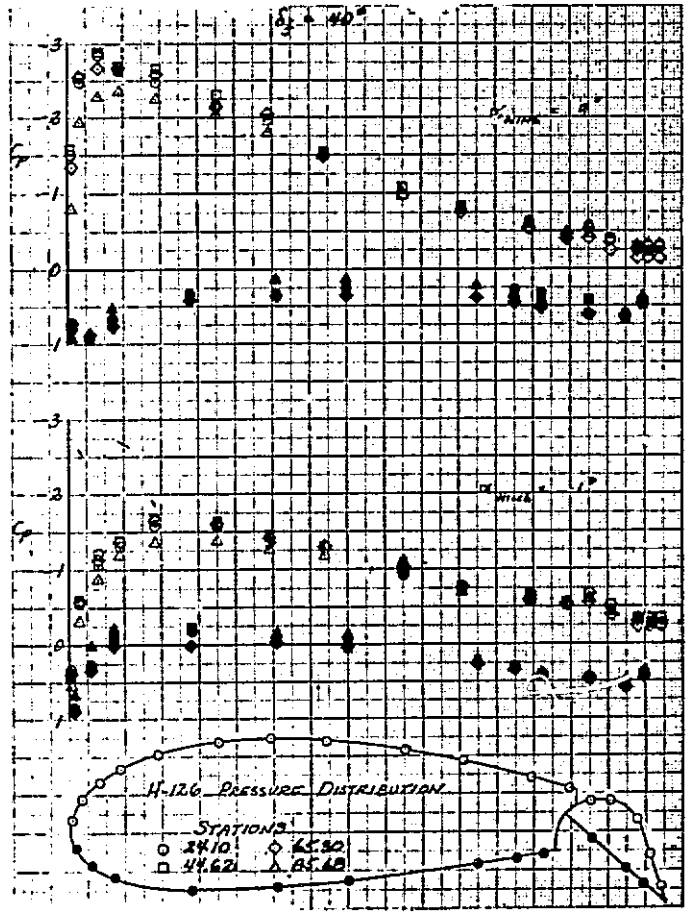

(b) $\delta_f = 40°$.

Figure 12. - Wing Pressure Distributions at $C_{J_W} = 0$.

(a) $\alpha = 0°$.

Figure 13. - Effect of C_{J_w} on Wing Pressure Distributions.

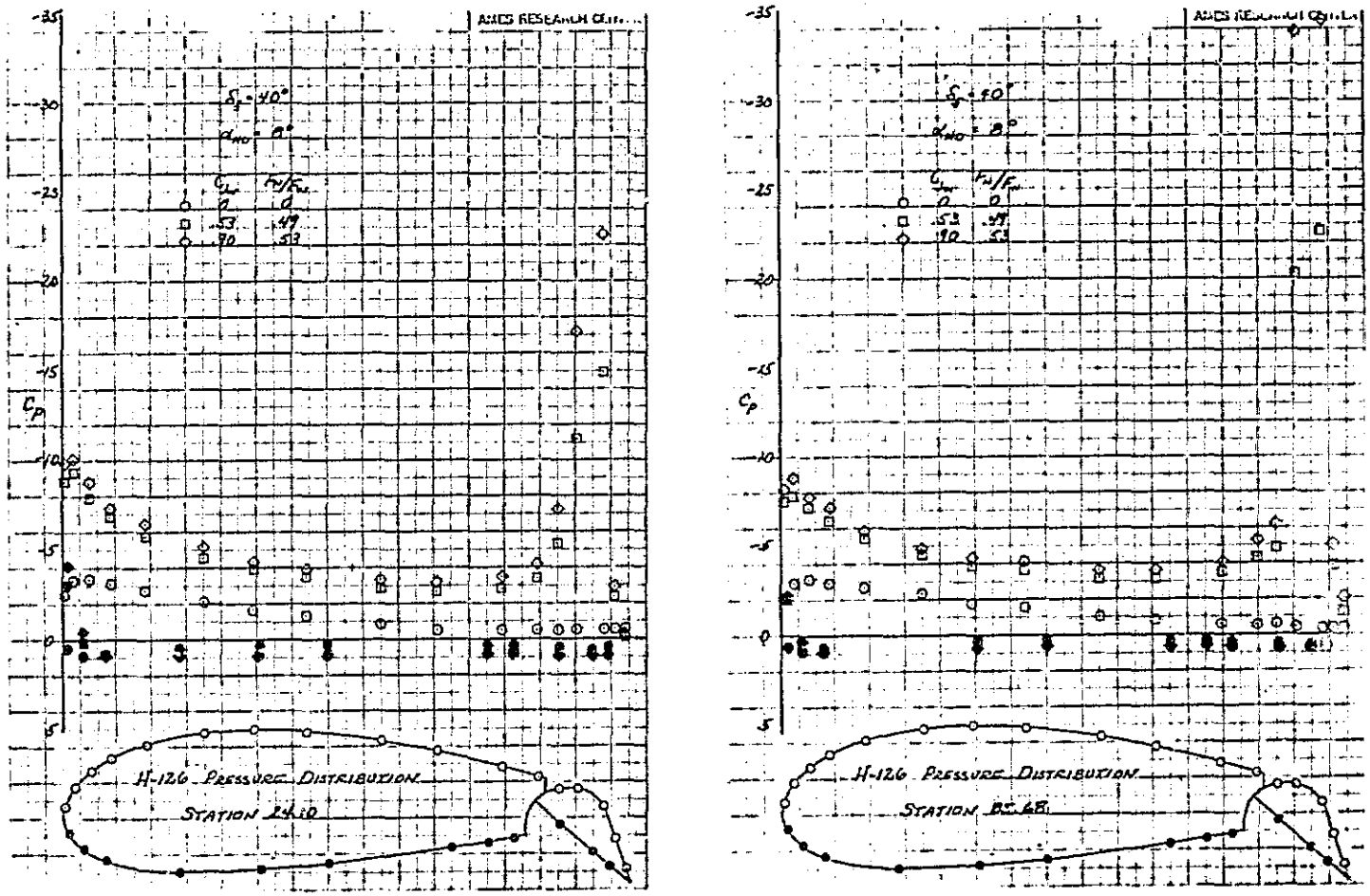

(b) $\alpha = 8°$.

Figure 13. - Concluded.

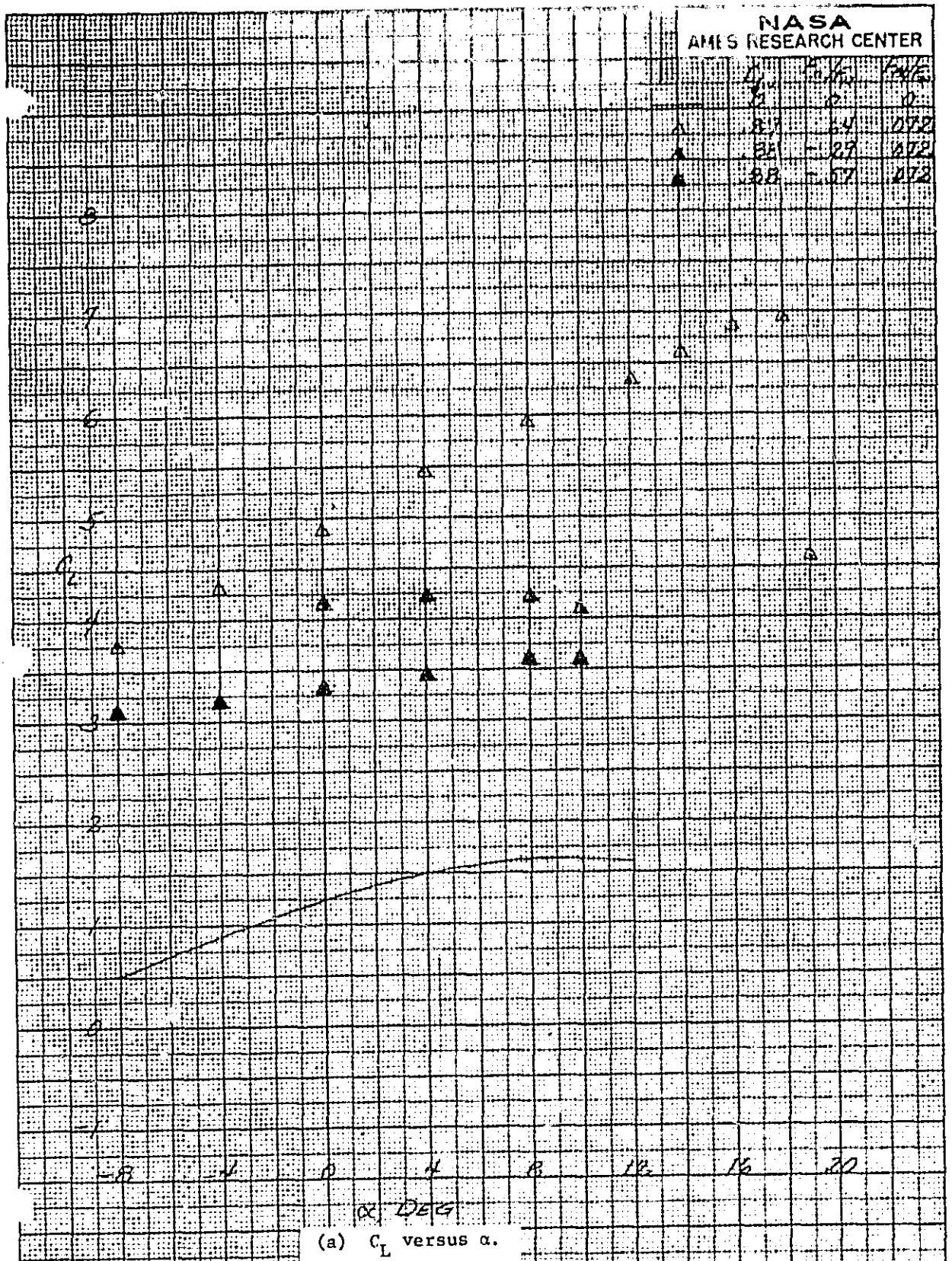

(a) C_L versus α.

Figure 14. – Model Longitudinal Characteristics with Modified Nozzle in Forward Location. $\delta_f = 40°$.

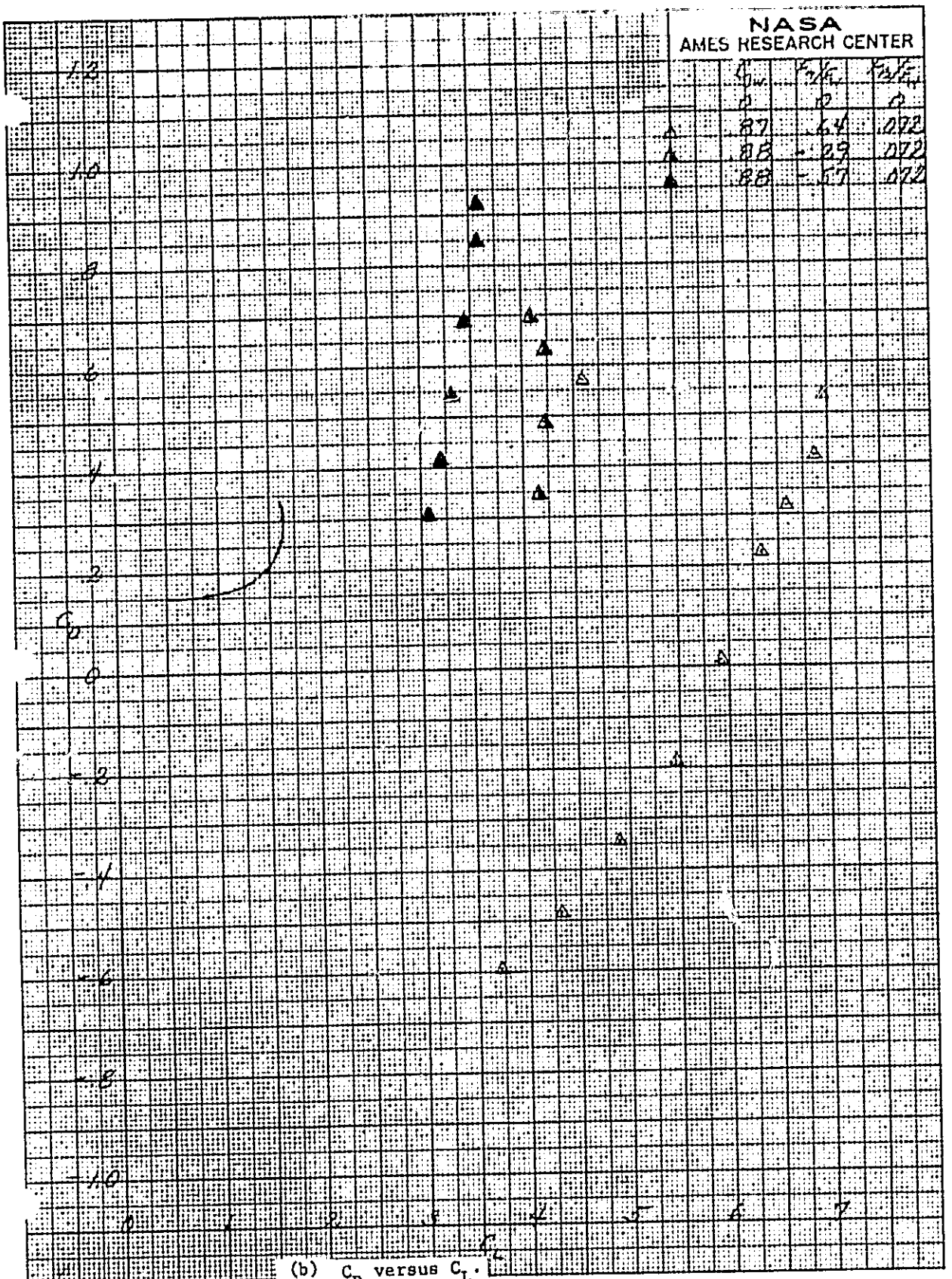

(b) C_D versus C_L.

Figure 14. - Continued.

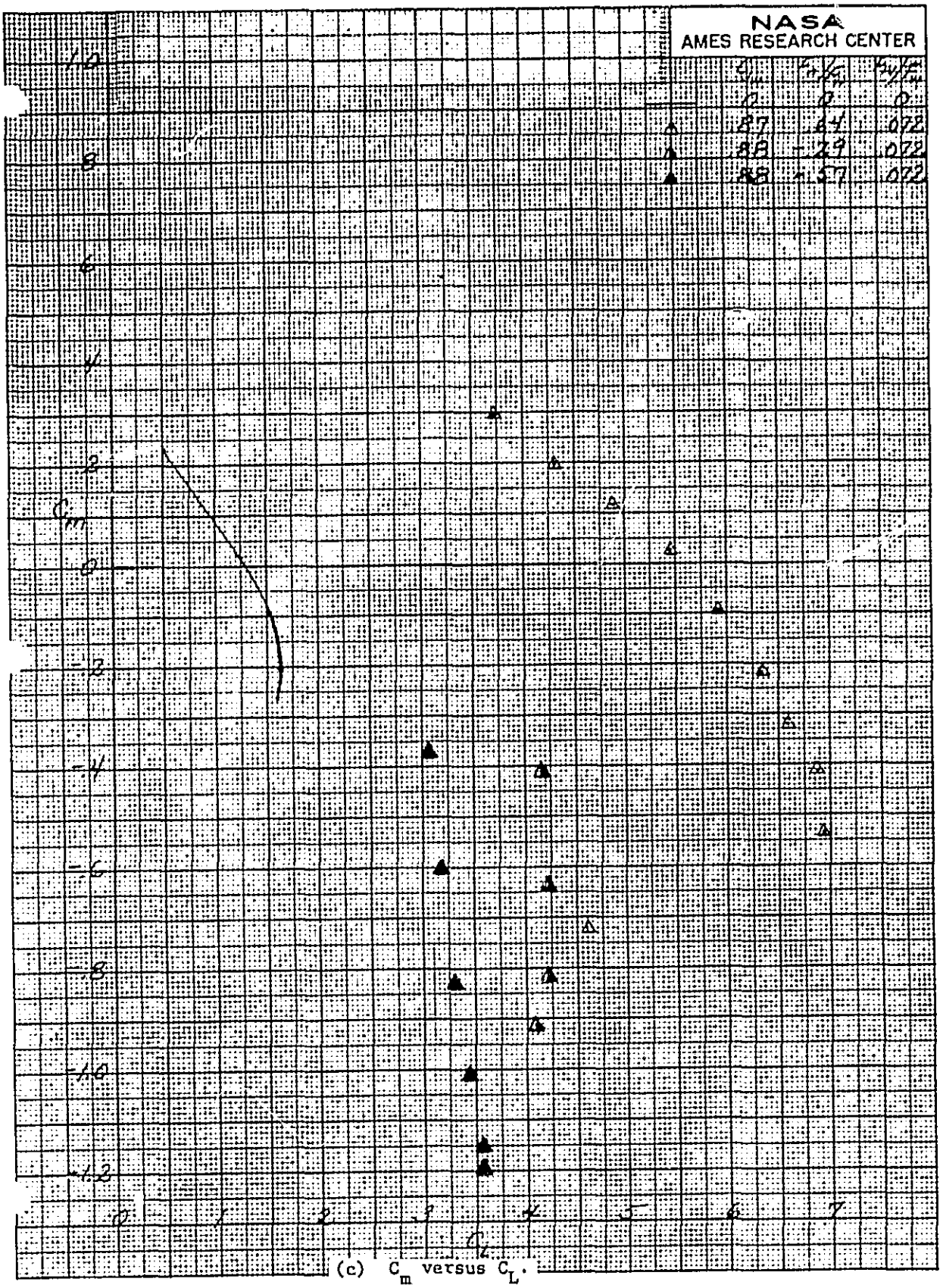

(c) C_m versus C_L.

Figure 14. - Concluded.

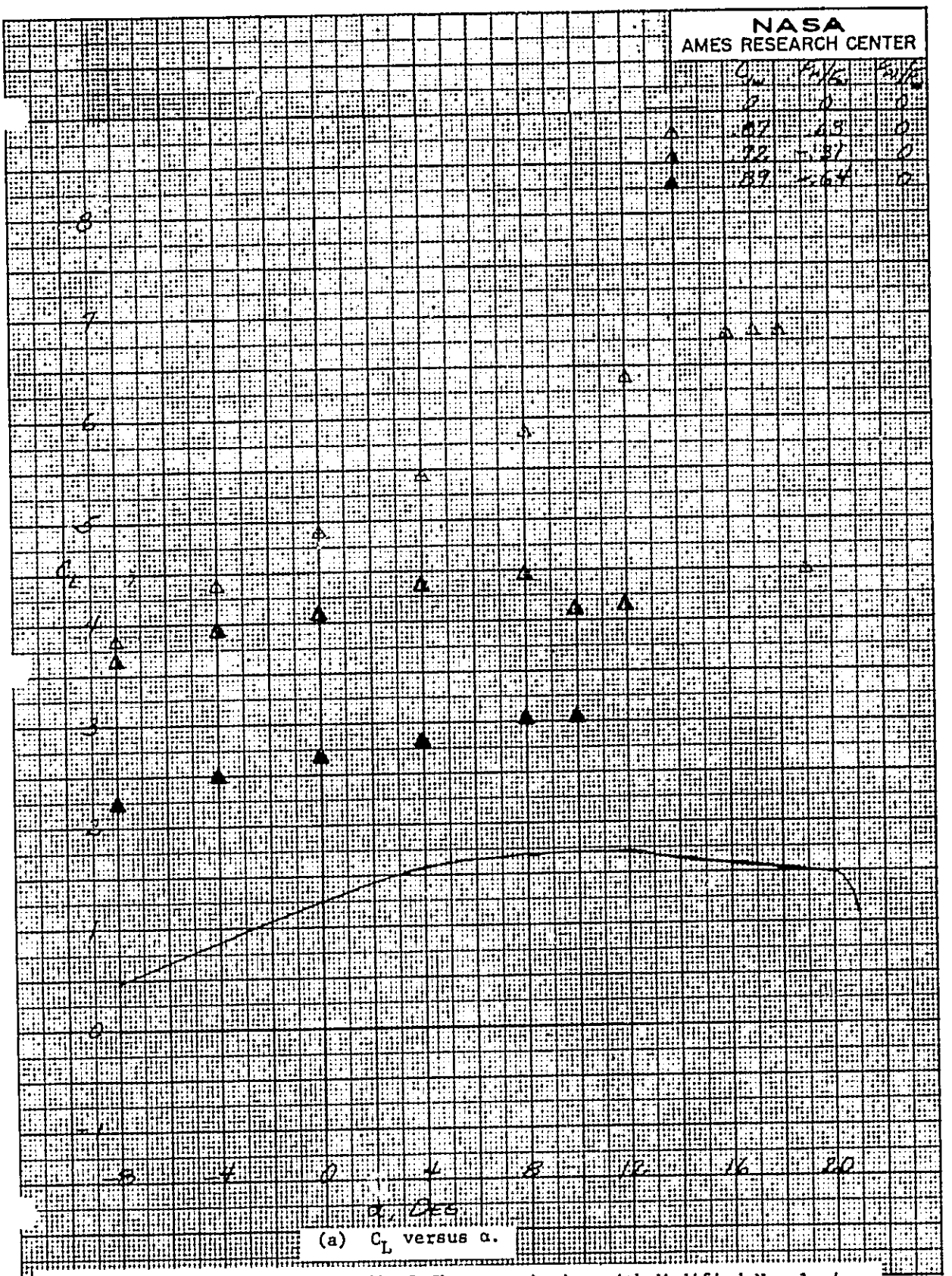

(a) C_L versus α.

Figure 15. – Model Longitudinal Characteristics with Modified Nozzle in Aft Location. $\delta_f = 40°$.

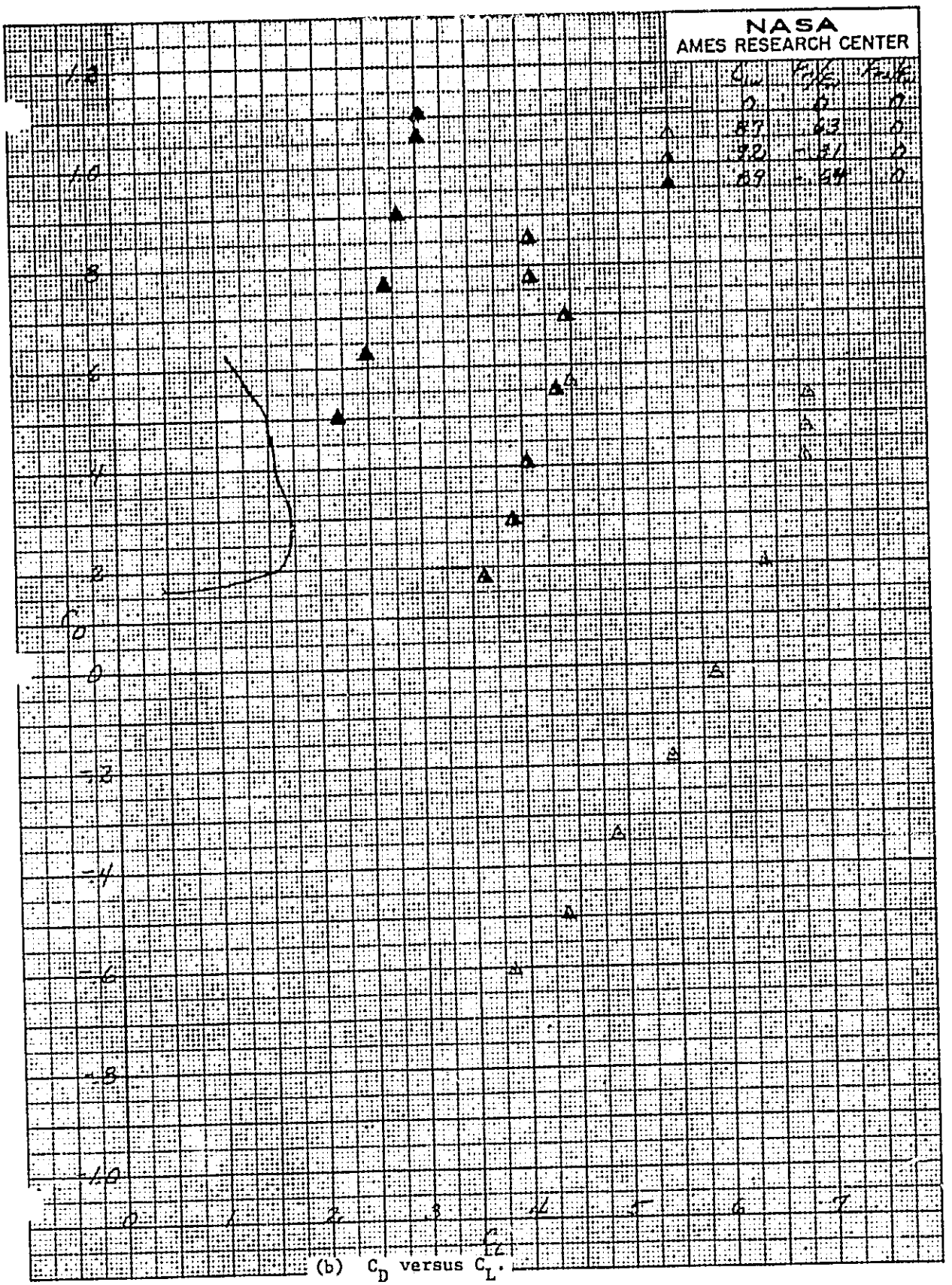

(b) C_D versus C_L.

Figure 15. - Continued.

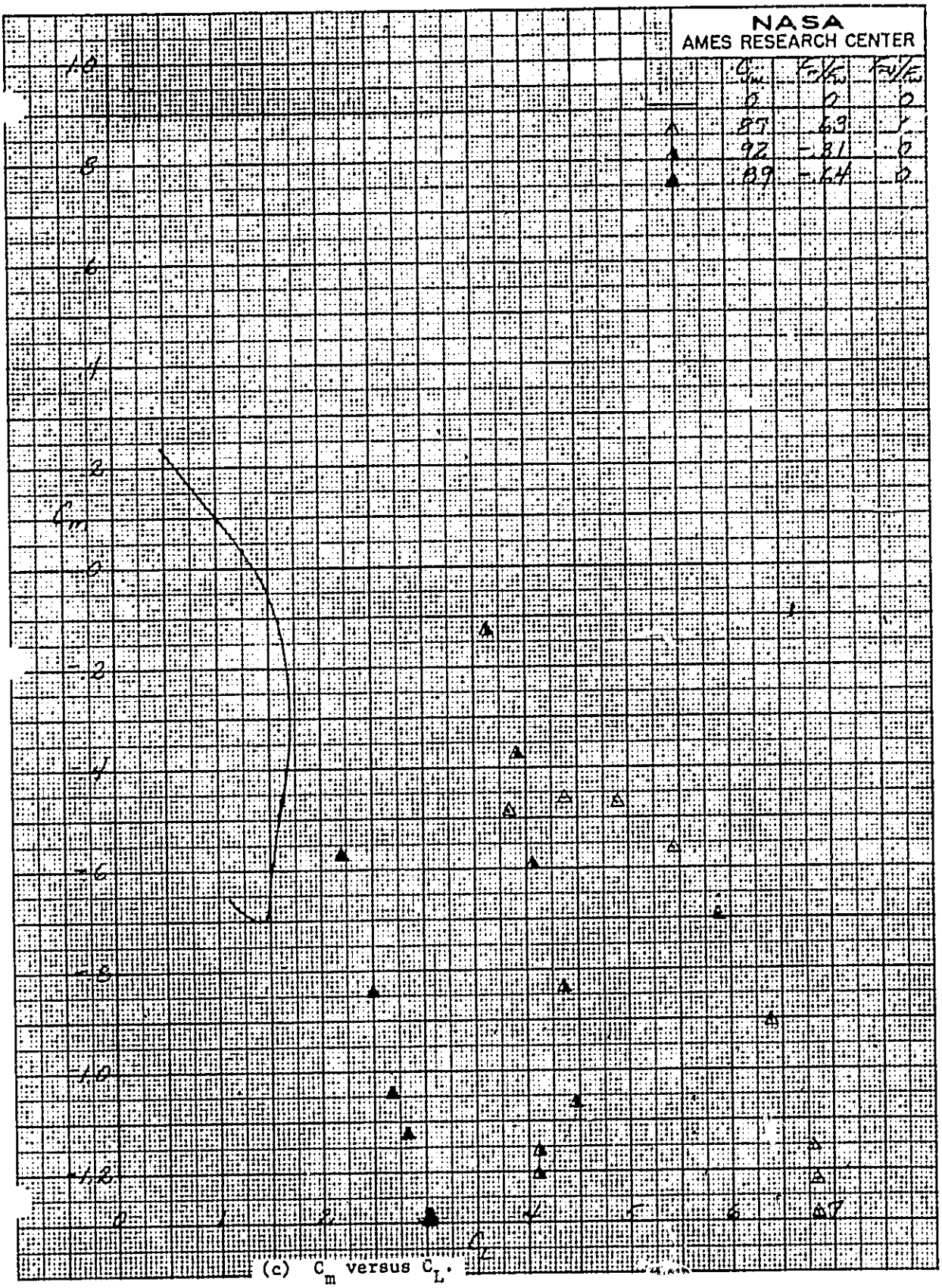

(c) C_m versus C_L.

Figure 15. - Concluded.

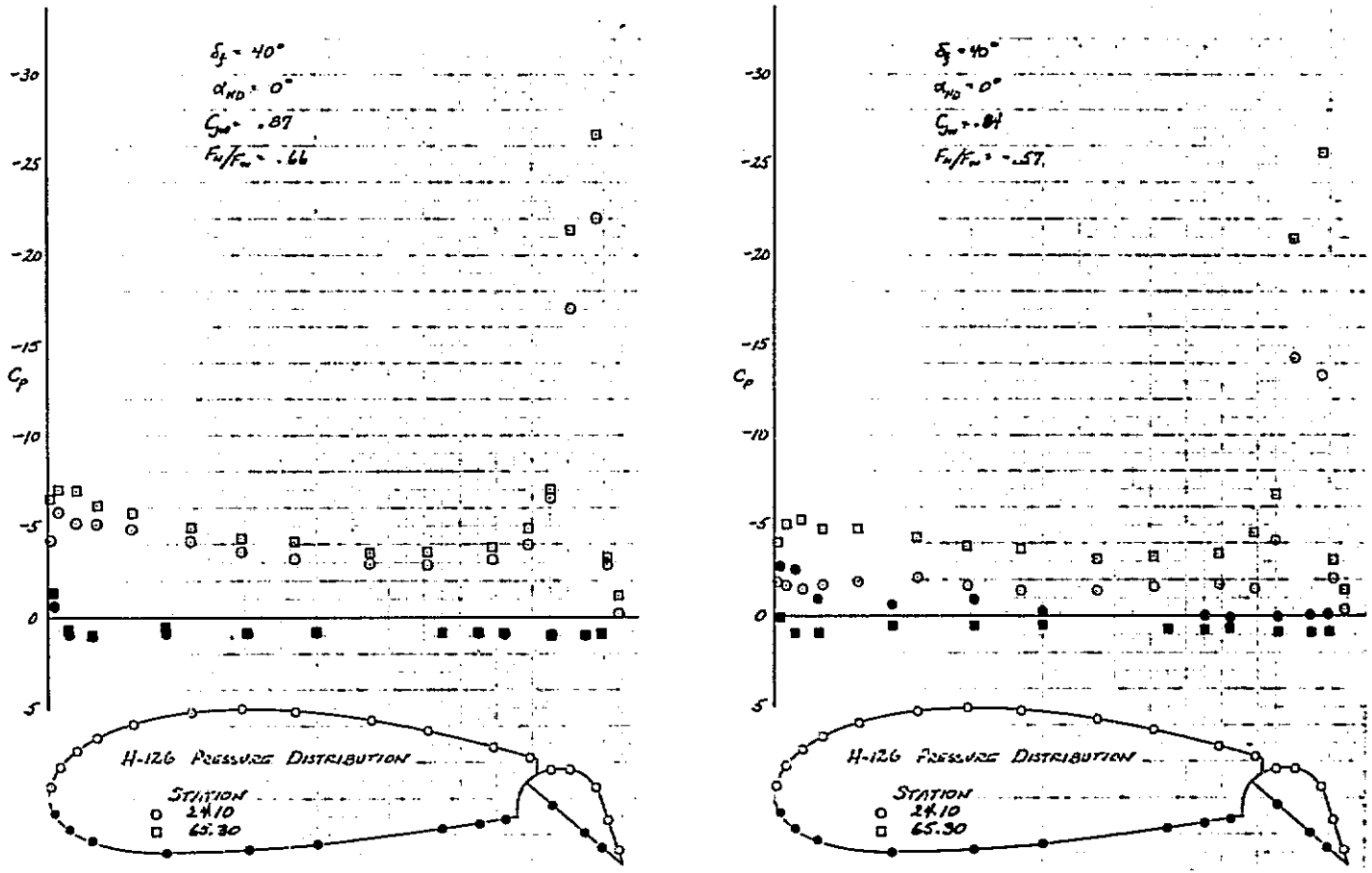

(a) Thrust Mode.

(b) Reverse Thrust Mode.

Figure 16. - Pressure Distributions Showing Effect of Reverse Flow Interference From Modified Fuselage Thrust Nozzle in Forward Location.

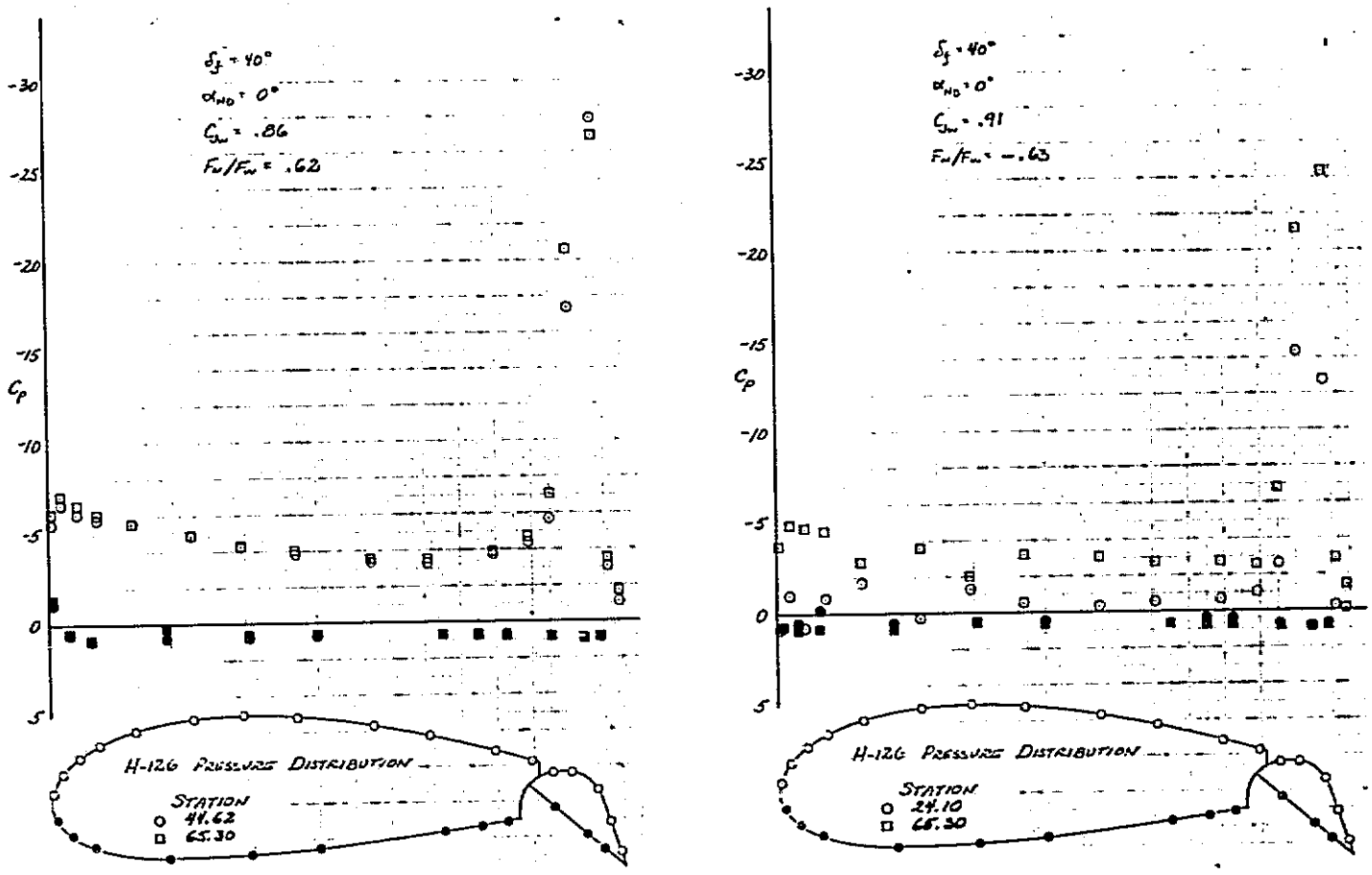

(a) Thrust Mode.

(b) Reverse Thrust Mode.

Figure 17. - Pressure Distributions Showing Effect of Reverse Flow Interference From Modified Fuselage Thrust Nozzle in Aft Location.

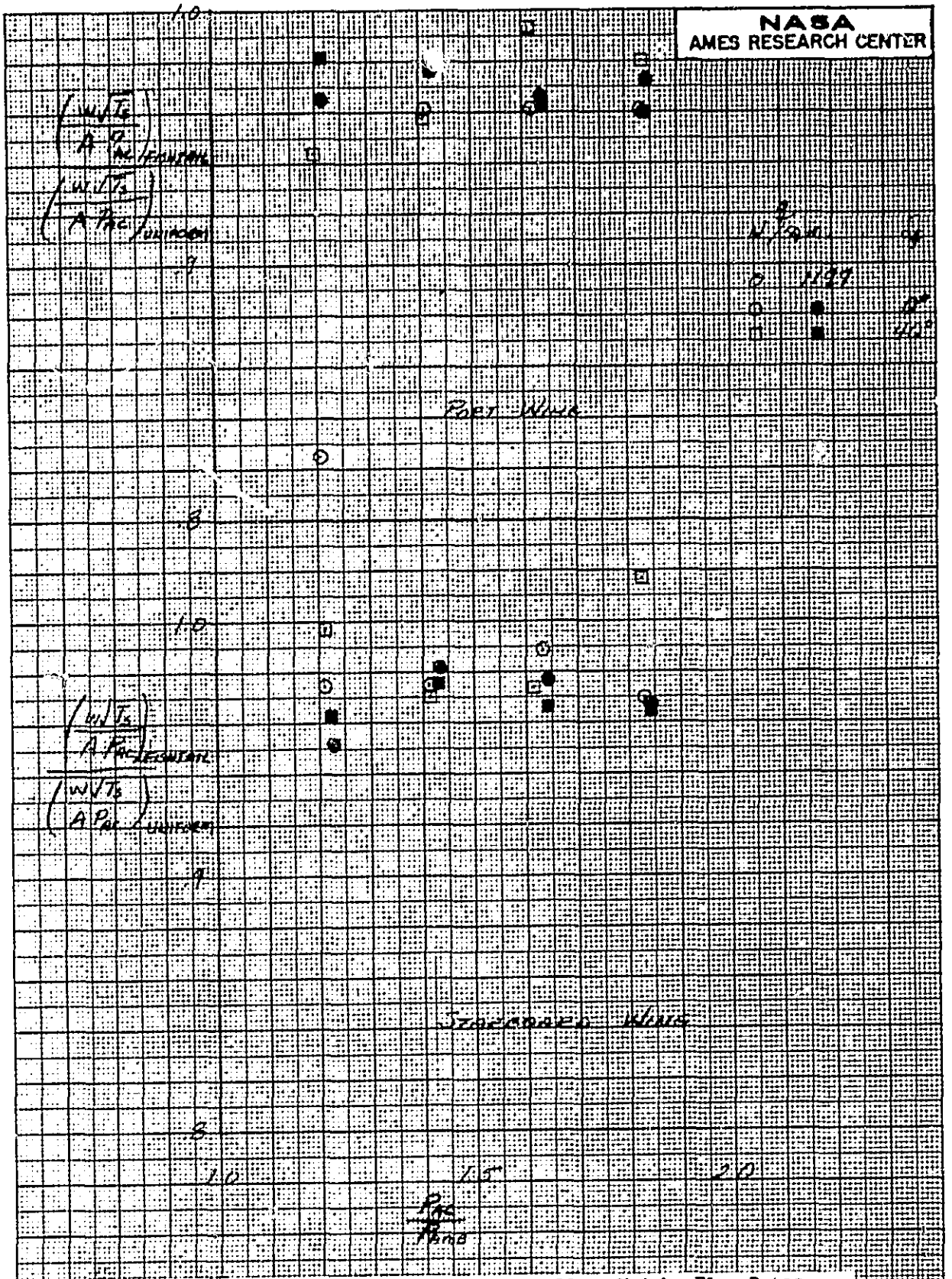

Figure 18. - Comparison of Wing Jet Efflux Weight Flow Rates.